NASA

MEMORANDUM

EVALUATION OF SEVERAL APPROXIMATE METHODS FOR CALCULATING THE SYMMETRICAL BENDING-MOMENT RESPONSE OF FLEXIBLE AIRPLANES TO ISOTROPIC ATMOSPHERIC TURBULENCE

By Floyd V. Bennett and Robert T. Yntema

Langley Research Center
Langley Field, Va.

NATIONAL AERONAUTICS AND SPACE ADMINISTRATION
WASHINGTON
March 1959

NASA MEMO 2-18-59L

NATIONAL AERONAUTICS AND SPACE ADMINISTRATION

MEMORANDUM 2-18-59L

EVALUATION OF SEVERAL APPROXIMATE METHODS FOR CALCULATING THE SYMMETRICAL BENDING-MOMENT RESPONSE OF FLEXIBLE AIRPLANES TO ISOTROPIC ATMOSPHERIC TURBULENCE

By Floyd V. Bennett and Robert T. Yntema

SUMMARY

Several approximate procedures for calculating the bending-moment response of flexible airplanes to continuous isotropic turbulence are presented and evaluated. The modal methods (the mode-displacement and force-summation methods) and a matrix method (segmented-wing method) are considered. These approximate procedures are applied to a simplified airplane for which an exact solution to the equation of motion can be obtained. The simplified airplane consists of a uniform beam with a concentrated fuselage mass at the center. Airplane motions are limited to vertical rigid-body translation and symmetrical wing bending deflections. Output power spectra of wing bending moments based on the exact transfer-function solutions are used as a basis for the evaluation of the approximate methods. It is shown that the force-summation and the matrix methods give satisfactory accuracy and that the mode-displacement method gives unsatisfactory accuracy.

INTRODUCTION

Current analytic methods of studying airplane responses to continuous atmospheric turbulence make use of the techniques from random-process theory. These techniques provide a compact description of the statistical properties of the turbulent velocities in a form suitable for response calculations. The significant characteristics of turbulence velocities for this purpose are contained in power spectra and appropriate cross-spectra. These spectra are then used along with the appropriate airplane frequency-response or transfer functions for determination of the airplane response.

The early applications of this technique described the turbulence as a one-dimensional random process varying along the flight path of the airplane but uniform along the wing span. (See, for example, ref. 1.) In recent studies the variation of turbulence across the wing span

(two-dimensional or isotropic turbulence) has been shown to give rise to significant effects for large flexible airplanes. (See, for example, ref. 2.)

In general, the solution of the dynamic equations of motion for the transfer functions requires the use of approximate procedures. It is the purpose of the present report to investigate the accuracy of several of these approximate procedures used for calculating the bending-moment transfer functions when applied to the case of a flexible airplane subjected to two-dimensional turbulence. The approximate methods under consideration are the mode-displacement method, the force-summation method, and a matrix method (segmented-wing method - also referred to as lumped-parameter method). An account of these approximate procedures can be found in reference 3, which also cites other references.

The approximate procedures under investigation are applied to a simplified airplane for which an exact solution to the equation of motion can be obtained. These exact-solution results serve as a basis for the evaluation of the approximate methods. For purposes of comparison, results are also calculated for the flexible airplane traversing one-dimensional turbulence and a rigid airplane traversing one- and two-dimensional turbulence.

The simplified airplane consists of a uniform beam with a concentrated fuselage mass at the center. Airplane motions are limited to vertical rigid-body translation and symmetrical wing bending deflections only. Aerodynamic forces are based on strip theory and include the effects of unsteady lift associated with the gusts and the resulting wing motions.

A secondary purpose of this report is to indicate some effects of spanwise variations of turbulence in addition to those given in reference 4. This purpose is accomplished by comparing mean-square bending-moment responses of various airplane configurations to one- and two-dimensional turbulence. The airplane configurations are defined by the ratio of fuselage mass to total mass.

SYMBOLS

b	wing span, ft
$C(k)$	generalized Theodorsen function
C_{L_α}	wing lift-curve slope per radian

c local wing chord, ft

$\bar{c}$ average chord, ft

c_{l_α} section lift-curve slope per radian

EI bending stiffness of wing, lb/sq ft

$F(k)$, $G(k)$ real and imaginary parts of generalized Theodorsen function $C(k)$, respectively

$H(k)$ transfer function of bending moment for one-dimensional turbulence

$H(k,\eta)$, $H(k,\eta+\theta)$ influence transfer functions of bending moment for two-dimensional turbulence

H_0 transfer function of bending moment resulting from vertical wing motion in rigid-body mode

H_1 transfer function of bending moment resulting from vertical wing motion in fundamental wing bending mode

H_2 transfer function of bending moment resulting from external gust loading

$K_0(\ )$, $K_1(\ )$ Bessel functions of second kind, order 0 and 1

k reduced frequency, $\frac{\omega\bar{c}}{2U}$

k_1 reduced frequency associated with fundamental wing bending mode, $\frac{\omega_1\bar{c}}{2U}$

$$k_a = \sqrt{\frac{(\bar{c}/2)^2 EI}{(b/2)^3 U^2 (m_w/2)}}$$

L scale of turbulence, ft

l_g gust load per unit span

l_i inertia load per unit span

l_m aerodynamic load per unit span due to wing vertical motion

M_B bending moment, ft-lb

$M_{B,s}$ bending moment due to sharp-edge gust, $\frac{1}{2} C_{L_\alpha} q S y_{cp} \frac{w}{U}$, ft-lb

$m(y)$ wing mass distribution, slugs/ft

m_F fuselage mass, slugs

m_W wing mass, slugs

$m_t(y)$, $m_t(\bar{y})$ total airplane mass distributions, slugs/ft

m_t total airplane mass, slugs

q dynamic pressure, lb/sq ft

R ratio of fuselage mass to wing mass, $\frac{m_F}{m_W} = \frac{\mu}{1 - \mu}$

$Re(\ )$ designates real part of ( )

S wing area, $\bar{c}b$, sq ft

s dimensionless scale of chordwise turbulence, $\frac{L}{\bar{c}/2}$

t time, sec

U forward velocity, fps

w vertical component of gust velocity, fps

y spanwise displacement, ft

$\bar{y}$ dimensionless spanwise displacement, $\frac{y}{b/2}$

y_{cp} lateral ordinate of center of pressure, $\frac{b}{2}\left(\frac{1}{2} - \bar{y}_1 + \frac{1}{2} \bar{y}_1^2\right)$, ft

$\bar{y}_{cp} = \frac{y_{cp}}{b/2}$

y_1 spanwise location of bending-moment station, ft

$\bar{y}_1$ dimensionless spanwise location of bending-moment station, $\frac{y_1}{b/2}$

z vertical displacement, ft

$\bar{z}$ dimensionless vertical displacement, $\frac{z}{c/2}$

$\Gamma(\theta)$ gamma function (see eq. (13))

$\gamma_n(\ )$ space function used in equation (9)

$\delta(\ )$ Dirac delta function

η, η_1 spanwise coordinates, ft

$\bar{\eta}$ dimensionless spanwise coordinate, $\frac{\eta}{b/2}$

θ variable of integration, $\eta_1 - \eta$, ft

κ airplane mass parameter, $\frac{\delta m_t}{C_{L_\alpha} \rho S c}$

κ_w wing mass parameter, $\frac{\delta m_w}{C_{L_\alpha} \rho S c} = \kappa(1 - \mu)$

μ fuselage mass ratio, $\frac{m_F}{m_t}$

$\xi_0(\ )$ rigid-body mode

$\xi_1(\ )$ fundamental wing bending mode

ρ air density, slugs/cu ft

σ^2 mean-square deviation of bending moment, lb-ft

$\Phi_{MB}(k)$ output power spectrum of bending moment

$\Phi_w(k)$ power spectrum of vertical gust velocity for one-dimensional turbulence

$\Phi_w(k,\theta)$, $\Phi_w(k,\eta_1-\eta)$ power spectra of vertical gust velocity for two-dimensional turbulence

$\Phi_{w_{mn}}(k)$ associated gust spectra (see eq. (12))

$\phi(k)$ unsteady lift function for gust penetration (Sears function)

ω frequency, radians/sec

ω_1 frequency associated with fundamental wing bending mode, radians/sec

$1(\ )$ unit step function

Subscripts:

f flexible airplane

I imaginary component of complex variable

n, m integers, 0, 1, 2, . . .

R real component of complex variable

Ra Rayleigh

r rigid airplane

Notation:

$*$ complex conjugate

$|\ |$ absolute value

$[\ ]$ square matrix

$\lceil\ \rfloor$ diagonal matrix

$\lfloor\ \rfloor$ row matrix

$\{\ \}$ column matrix

A dot over a symbol indicates a derivative with respect to time, and a prime indicates a derivative with respect to y.

BASIC INPUT-OUTPUT RELATIONS

Random-process techniques as applied to the gust-load problem are discussed in many references. (For example, see refs. 1 to 4.) From reference 4, the output spectra of bending moments are defined as follows:

For one-dimensional turbulence,

$$\Phi_{MB}(k) = \left|H(k)\right|^2 \Phi_w(k) \tag{1}$$

where

$\Phi_{MB}(k)$ output power spectrum of bending moment

$H(k)$ transfer function for bending-moment response of airplane to continuous sinusoidal gusts of unit amplitude and wave length $\pi c/k$

$\Phi_w(k)$ input power spectrum of vertical gust velocity

For two-dimensional turbulence,

$$\Phi_{MB}(k) = \int_{-b/2}^{b/2}\int_{-b/2}^{b/2} H(k,\eta)H^*(k,\eta_1)\Phi_w(k,\eta_1-\eta)\,d\eta\,d\eta_1 \tag{2}$$

where

$H(k,\eta)$ influence transfer function which represents the complex amplitude of bending-moment response to continuous sinusoidal gust of unit amplitude and wave length $\pi c/k$ impinging at station η (* indicates complex conjugate)

$\Phi_w(k,\eta_1-\eta)$ input power spectrum of vertical gust velocity

It has been shown in reference 4 that equation (2) may be simplified somewhat by a change of variable; namely, $\eta_1 = \theta + \eta$. Thus, performing the integrations first over η and then over θ, as shown in reference 4, and restricting the system to the symmetrical response only yields

$$\Phi_{MB}(k) = \int_0^b \Phi_w(k,\theta)\,d\theta \int_{-b/2}^{\frac{b}{2}-\theta} \left[H_R(k,\eta)H_R(k,\eta+\theta) + H_I(k,\eta)H_I(k,\eta+\theta)\right] d\eta \tag{3}$$

where $H_R(\ )$ and $H_I(\ )$ are, respectively, the real and imaginary components of the symmetrical transfer functions.

The output spectra, defined by equations (1) and (3), can in turn be used to calculate many other statistical quantities (see ref. 5); however, the only other statistical quantity to be calculated herein is the mean-square deviation of the bending moment. From reference 4, the mean-square response is defined as

$$\sigma^2 = \int_0^\infty \Phi_{MB}(k)\,dk \tag{4}$$

TRANSFER FUNCTIONS

From simple beam theory, the basic differential equation of bending motion is

$$\frac{d^2}{dy^2}\left(EI\,\frac{d^2z}{dy^2}\right) = l_i + l_m + l_g \tag{5}$$

where l_i is the inertia load per unit span and l_g and l_m are, respectively, the aerodynamic loads per unit span due to the disturbing gust and those due to wing vertical motions.

Solutions of equation (5) to obtain airplane motions and deflections and, subsequently, the determination of the bending-moment transfer functions are accomplished by an exact method, two modal methods (mode displacement and force summation), and a matrix method (segmented-wing method).

All of the solutions are made for the simplified airplane, consisting of a uniform beam with a concentrated fuselage mass at the center, shown in figure 1. It is assumed that the airplane is restricted to vertical motions only and, in addition, that the pitching motions be neglected.

Exact Method

Equation (5) is solved by means of the Laplace transform method to obtain z'' and, thence, the bending-moment influence transfer function from EIz''. A brief derivation of the exact analysis is given in appendix A for one- and two-dimensional turbulence.

Modal Methods

The fundamental assumption in all modal methods is that the displacement can be approximated by the superposition of a finite number of natural or assumed mode shapes. This assumption allows equation (5) to be replaced by a set of equations of modal motion which can be solved for the displacement due to each mode. The bending-moment transfer function is then calculated by two methods: first, the mode-displacement method, in which the bending moment is determined directly from the curvature associated with the flexible mode-displacement response and, second, the force-summation method, in which the motion and aerodynamic loadings associated with the modal motions, rigid and flexible, are obtained first and then integrated with the applied gust loading to obtain the bending-moment response. Brief derivations of these modal analyses are given in appendix B for one- and two-dimensional turbulence.

Matrix or Segmented-Wing Method

Equation (5) is integrated twice to obtain an integral equation with z'' as the unknown. In order to solve this integral equation, the wing is divided into $n - 1$ segments; thus, the equation can be written as an nth-order matrix equation.

Integrating matrices of the type given in reference 6 are used to solve this matrix equation directly for z'' and, thence, the bending-moment transfer function from EIz''. A brief derivation of the matrix method is presented in appendix C for one- and two-dimensional turbulence.

INPUT SPECTRA

The input spectra required by equations (1) and (3) may be approximated by several analytic expressions. (See ref. 7.) The expressions used herein are:

For one-dimensional turbulence,

$$\Phi_w(k) = \frac{s}{\pi}\left[\frac{1 + 3s^2k^2}{\left(1 + s^2k^2\right)^2} + \frac{a^2 + 6s^2a^2k^2 - 3s^4k^4}{\left(a^2 + s^2k^2\right)^3}\right]\left(\frac{w}{U}\right)^2 \qquad (6)$$

For two-dimensional turbulence,

$$\Phi_w(k,\theta) = \frac{s}{\pi}\left(\frac{w}{\bar{U}}\right)^2\left[\frac{\left(1 + 3s^2k^2\right)\theta}{\left(1 + s^2k^2\right)^{3/2}} K_1\left(\theta\sqrt{1 + s^2k^2}\right) - \frac{\theta^2}{1 + s^2k^2} K_0\left(\theta\sqrt{1 + s^2k^2}\right) + \right.$$

$$\frac{2a^2\theta^2\left(a^2 + 3s^2k^2\right)}{\left(a^2 + s^2k^2\right)^2} K_0\left(\theta\sqrt{a^2 + s^2k^2}\right) +$$

$$\left.\frac{\left(a^4 + 6a^2s^2k^2 - 3s^4k^4\right)\theta - \left(a^2 + s^2k^2\right)a^4\theta^2}{\left(a^2 + s^2k^2\right)^{5/2}} K_1\left(\theta\sqrt{a^2 + s^2k^2}\right)\right] \tag{7}$$

where

s dimensionless scale of turbulence, $\frac{L}{\bar{c}/2}$

L longitudinal scale of turbulence

a arbitrary constant used to select frequency at which spectrum begins to deviate from an inverse second-power variation with frequency and begins to decrease more rapidly

On the basis of the measurements reported in reference 7, a value for a of 50 appears appropriate and is used in the present calculations. (Note that eq. (7) reduces to eq. (6) as $\theta \to 0$.)

DETERMINATION OF OUTPUT SPECTRA

For one-dimensional turbulence, the output spectrum is obtained simply and directly from equation (1) for all methods considered. For two-dimensional turbulence, however, it should be noted from equation (3) that a double integration of the product of the input spectrum and the convolution of the transfer function is necessary before the output spectrum can be evaluated. For the exact and matrix methods these integrations were performed numerically because of the complexity of the integrands. For the modal methods, however, equation (3) is simplified by the separation of the frequency and space variables in the transfer function; that is,

$$H(k,\eta) = \sum_{n=0}^{r-1} H_n(k)\gamma_n(\eta) \tag{9}$$

where r indicates the number of modes, including rigid-body modes, in the analysis. This separation of variables reduced equation (3) to the following form:

$$\Phi_{MB}(k) = \sum_{n=0}^{j} \sum_{m=0}^{j} \mathrm{Re}\left[H_m(k)H_n^*(k)\right]\Phi_{w_{mn}}(k) \tag{10}$$

where for mode-displacement method

$$j = r - 1$$

and for force-summation method

$$j = r$$

and

$$\Phi_{w_{mn}}(k) = \int_0^b \Gamma(\theta)\Phi_w(k,\theta)d\theta \tag{11}$$

$$\Gamma(\theta) = \int_{-b/2}^{b/2} \gamma_m(\eta)\gamma_n(\eta+\theta)d\eta \tag{12}$$

The force-summation method contains more terms than does the mode-displacement method due to the externally applied gust load. (See appendix B.) It should also be noted that the transfer function $H_n(k)$ is not identical in the two methods; for example, see equations (B11b) and (B15b).

The integrand of equation (12) is a relatively simple function and in most cases is integrated in closed form. However, the integration indicated in equation (11) is performed numerically because of the complexity of the input spectrum.

SCOPE OF CALCULATIONS

Output spectra and mean-square values of the bending-moment response at the wing root and the 0.75-semispan station for one- and two-dimensional

turbulence have been computed for three configurations of the simplified airplane (fig. 1). These configurations, defined by the variable μ, the ratio of fuselage mass to total mass, are:

$\mu = 0$ (all mass uniformly distributed across the wing span)

$\mu = 0.5$ (one-half the total mass concentrated in the fuselage and one-half uniformly distributed across the span)

$\mu = 0.8$ (80 percent of the mass concentrated in the fuselage and 20 percent distributed uniformly across the span)

In all computations, the aspect ratio was assumed to be 12.0, and the dimensionless scale of chordwise turbulence $s = \frac{L}{\bar{c}/2}$ was assumed to be 100. In order to facilitate the computations, the reduced frequency k_1 associated with the first free-free symmetrical mode of the dynamic system involving wing bending and the wing aerodynamic mass parameter κ_w were assumed to be invariant with μ. These assumptions reduced the computational labor appreciably but resulted in each of the three airplane configurations having a different total airplane mass. Since, however, the purpose of this study was to evaluate methods rather than to show trends, this difference was not considered a serious drawback.

The values chosen for the constants, $k_1 = 0.2$ and $\kappa_w = 100$, correspond to those of an aircraft which has a high degree of wing flexibility and low aerodynamic damping. Such a system, it was felt, would provide a severe test of the adequacy of the approximate methods to be evaluated. Since the wing mass parameter was held constant, the airplane aerodynamic mass parameter varied with μ - that is, for $\mu = 0$, $\kappa = 100$; for $\mu = 0.5$, $\kappa = 200$; and for $\mu = 0.8$, $\kappa = 500$.

Aerodynamic strip theory was used in all of the studies since a more refined theory would have further complicated the already complex solutions and probably would not have influenced appreciably the conclusions regarding the relative accuracy of the various methods. Also, the unsteady lifts associated with the gusts and the resulting wing motions were included in the analyses.

All the results presented herein are in nondimensional form. The output bending-moment spectra and the mean-square results have been divided by the square of the bending moment due to a sharp-edge gust of unit vertical velocity which is constant across the span.

The modal methods require a finite number of modes to approximate the airplane motions. For the mode-displacement method, rigid-body

translation and the first natural wing bending mode were used. For the force-summation method, the following three approximations were investigated:

(1) Rigid-body translation and the first natural wing bending mode (same as for the mode-displacement method)

(2) Rigid-body translation and a parabolic approximation to the first free-free wing bending mode

(3) Same as approximation (2) except that the frequency associated with the natural wing bending mode was used instead of the approximate Rayleigh frequency

The matrix method requires that the wing be divided into a number of equally spaced stations across the span in order to perform the matrix integrations. For the present study, five such stations across the wing semispan were used.

For purposes of comparison, bending-moment results were also calculated for the simplified airplane considered to be rigid. For these calculations the force-summation method was used with the airplane motions limited to rigid-body translation only. A brief derivation of this procedure is given in appendix D.

ACCURACY OF NUMERICAL INTEGRATIONS

Inasmuch as the integrations involved in calculating the two-dimensional output spectra were performed numerically (see the section entitled "Determination of Output Spectra"), a check on the numerical accuracy was deemed necessary.

Exact Method

For the exact method a suitable check on the numerical accuracy of the two-dimensional expression was obtained by calculating the one-dimensional output spectra from the two-dimensional expression (see eq. (3)) and comparing the results with those from the one-dimensional expression (eq. (1)). This one-dimensional check calculation is obtained by substituting $\Phi_w(k)$ for $\Phi_w(k,\theta)$ in equation (3). Thus, any discrepancies between the results of the two procedures can be traced directly to the numerical integrations of the two-dimensional expression. A comparison of these results is given in figure 2.

From part (a) of figure 2 it is evident that both methods give nearly the same results for the spectra of root bending moment. It can, therefore, be expected that the accuracy of the root-bending-moment results for the two-dimensional gust structure are satisfactory.

From part (b) of figure 2 it is evident that both methods do not give the same results for the spectra of bending moment at the 0.75-semispan station. It can, therefore, be expected that the results at the 0.75-semispan station for the two-dimensional gust structure will not be very accurate. The inaccuracy of these results can, in large part, be attributed to the fact that the 0.75-semispan station is located between two of the equally spaced stations used in the numerical integration procedures. This location, unfortunately, places the numerous discontinuities in the slope of the transfer functions (see fig. 3) to be integrated midway between the stations. At the time of this discovery it was considered impractical to change to another spanwise station; thus, the results at the 0.75-semispan station calculated by the exact method will not be presented for the two-dimensional turbulence condition.

Modal Methods

For the modal methods the integrations to be performed in order to evaluate the output spectra are defined by equations (11) and (12). The first integration, equation (12), is of a form which can be integrated analytically or accurately by numerical procedures. Thus, the subsequent integration, equation (11), which is performed numerically, should also be accurate.

Matrix Method

The numerical integrations used to calculate output spectra for the matrix method are the same as those used in the exact method. Figure 3 shows that excellent agreement exists between the exact and matrix transfer functions; thus, the numerical inaccuracies in this method are predominantly the same as in the exact approach. For this reason, the matrix results at the 0.75-semispan station for two-dimensional turbulence are not presented.

EVALUATION OF APPROXIMATE PROCEDURES

In this section the various approximate procedures are evaluated from the output-spectra and mean-square bending-moment results for one- and two-dimensional turbulence. In order to facilitate the discussion, the approximate procedures are divided into two groups: first, the more

accurate methods consisting of the force-summation method based on a natural mode and the matrix method; second, several simplified modal methods consisting of the mode-displacement method based on a natural mode and the force-summation method based on a parabolic mode with the corresponding Rayleigh-Ritz frequency and with the natural frequency.

For all solutions the results for the three model configurations studied show the same type of comparison; thus, the output spectra are presented for only one representative configuration, namely, $\mu = 0.5$.

Force-Summation and Matrix Methods

Statistical bending-moment results obtained by the force-summation method using one natural mode and the five-station matrix method are evaluated by comparison with the exact-method results. In order to permit evaluation of the influence of the second symmetrical bending-moment resonance peak on the results, the output spectra have been calculated by the exact and the matrix methods over a larger range of reduced frequencies than is usually considered necessary. The output spectrum for the airplane assumed to be rigid is also presented for comparison.

Bending moment at the wing root.- Spectra of the bending moment at the wing root for a one-dimensional gust structure are presented in figure 4(a). It is readily apparent that both of the approximate methods yield spectra which are almost the same as those for the exact-method results. Also, the results for the rigid airplane agree very well with the results for the flexible airplane calculated by the exact method for small values of the reduced frequency where dynamic flexibility effects are unimportant.

Spectra of the bending moment at the wing root are compared in figure 4(b) for the case of a two-dimensional gust structure. The agreement is again seen to be very good throughout the frequency range.

For both the one-dimensional and the two-dimensional gust structures, the peak of second symmetrical bending mode, located at $k = 1.12$, is so small that it is barely evident on the plots and, thus, has little effect on mean-square results.

Bending moment at 0.75-semispan station.- Spectra of the bending moment at the 0.75-semispan station for a one-dimensional gust structure are compared in figure 4(c). The two approximate solutions agree very well with the exact-method results. The force-summation solution, of course, does not give the second-mode resonant peak, and the matrix method gives it displaced to a somewhat higher frequency. In this high frequency range there is no experimental confirmation of the shape of the input gust spectrum; thus, the significance of the second-mode peak

is questionable. For mean-square results this peak can be neglected, but for higher statistical moments, such as are needed to predict the time expected to exceed a given bending-moment level, these secondary peaks may be important.

For the two-dimensional case it was found that the exact- and matrix-method results for the 0.75-semispan station were inaccurate due to numerical integrations. (See section entitled "Accuracy of Numerical Integrations.") Hence, figure 4(d) presents only the force-summation and rigid-airplane results. Since the numerical integration errors present in the exact and matrix methods are not present in the force-summation method, there is no reason to believe that this method is any less accurate for this case than for any other case considered. Figure 4(d) lends support to this statement, by showing good agreement between the force-summation method and the rigid analysis at low frequencies. It should be remembered that the numerical inaccuracies in the exact and matrix methods occurred in the determination of the output spectra and not in the transfer-function calculations. Thus, as was shown in figure 3, the matrix method yields excellent two-dimensional transfer-function results.

Simplified Modal Methods

Statistical bending-moment results obtained by simplified modal approaches are evaluated by comparison with the force-summation results based on a natural mode. (This method has been shown to be accurate in the preceding section.) The simplified modal methods consist of the mode-displacement method based on a natural mode and the force-summation method based on an approximate parabolic mode. Two different procedures are used in the latter method: the Rayleigh-Ritz procedure in which the Rayleigh frequency associated with the approximate mode is used, and the modified Rayleigh-Ritz procedure in which the frequency associated with the natural mode is used.

Bending moment at the wing root.- Spectra of the bending moment at the wing root calculated by the modal methods for a one-dimensional gust structure are shown in figure 5(a). Compared with the force-summation method based on a natural mode, the mode-displacement method yields inaccurate results in the low frequency range. The force-summation Rayleigh-Ritz approach based on the parabolic mode results in a shift of the resonance peak, as would be expected, because of the Rayleigh frequency. Although, this approach yields a fairly good result for the mean-square bending moment, it would be a very poor choice if higher statistical moments were desired. The force-summation modified Rayleigh-Ritz approach based on the parabolic mode is almost as accurate as the results when the natural mode is used.

The results for the two-dimensional gust structure are presented in figure 5(b). The same trends can be seen as for the one-dimensional case.

Bending moment at the 0.75-semispan station.- Spectra of the bending moment at the 0.75-semispan station obtained by the modal methods are shown in figures 5(c) and 5(d) for the one- and two-dimensional gust structure, respectively. It is again apparent that the mode-displacement method is very inaccurate in the low frequency range, whereas the force-summation modified Rayleigh-Ritz approach is very accurate throughout the frequency range shown. Results were not calculated by the force-summation Rayleigh-Ritz approach based on the parabolic mode for this station.

EFFECTS OF SPANWISE VARIATIONS OF TURBULENCE

In this section the effect of the spanwise variation of vertical turbulence on the bending-moment response is assessed. First, the effects on the output spectra are shown in figure 6. Part (a) of this figure shows the spectra at the wing root as determined by the exact method. For the configurations with $\mu = 0.5$ and 0.8, it is apparent that the main effect of the spanwise variation of turbulence is an appreciable reduction in the bending-moment response as compared with the one-dimensional case, particularly in the vicinity of the fundamental mode resonant peak. For the configuration with $\mu = 0$, however, the two-dimensional turbulence results in an increase in root-bending-moment response because the response produced by the one-dimensional turbulence is zero. Part (b) of figure 6 shows the spectra at the 0.75-semispan station as determined by the force-summation method. (The exact-method results have been shown to be inaccurate for this station because of numerical integrations.) The same results are apparent at this station as at the root station.

Second, the effects of spanwise variations of turbulence on the mean-square bending-moment results are shown in figure 7. As would be expected, the same effects shown on the spectra are further amplified in the mean-square results; namely, a decreased response for $\mu = 0.5$ and 0.8 and an increased response for $\mu = 0$. These results are in agreement with those given in reference 4 for root-bending-moment response.

Finally, the effects of spanwise variations of turbulence on an amplification factor, defined as the ratio of the mean-square bending moment of the flexible airplane to the mean-square bending moment of the rigid airplane, are shown in figure 8. Again the same general conclusions that were reached for the results shown in figures 6 and 7 are evident. In addition, it should be noted in the low μ range $(\mu \to 0)$ that the trend of the amplification factors for the one-dimensional gust is not the same as that for the more realistic two-dimensional gust.

CONCLUSIONS

A study has been made of the relative accuracy of several approximate procedures for calculating the symmetrical bending-moment response of flexible airplanes to continuous isotropic turbulence. These approximate procedures have been applied to a simplified airplane which consists of a uniform beam with a concentrated fuselage mass at the center. The conclusions drawn from this study are:

1. The force-summation method based on one natural bending mode gives very good results compared with the exact solution.

2. The matrix method based on five stations across the semispan gives very good results compared with the exact solution.

3. The mode-displacement method based on a natural mode yields inaccurate results; however, this relatively simple method can be useful in trend studies involving variations in wing flexibility.

4. The force-summation method, based on an approximate parabolic mode and the Rayleigh frequency, loses little accuracy in mean-square results. However, the approximated natural frequency causes a shift in the fundamental mode resonant peak; consequently, higher statistical moments will be in appreciable error.

5. The force-summation method based on an approximate parabolic mode loses little accuracy if the natural frequency is known.

In addition to the evaluation of approximate methods, the effects of spanwise variations of vertical gust velocity were also studied. From this study it was found that the inclusion of spanwise variations of turbulence results in a decreased response if most of the airplane mass is in the fuselage and in an increased response if most of the mass is in the wing. Also, the exclusion of spanwise variations of turbulence in trend studies, such as the trend of amplification factor with mass ratio, may lead to erroneous conclusions.

Langley Research Center,
National Aeronautics and Space Administration,
Langley Field, Va., October 24, 1958.

APPENDIX A

EXACT ANALYSIS FOR SIMPLIFIED MODEL SUBJECTED TO SYMMETRICAL PART OF RANDOM-GUST DISTURBANCES

The differential equation defining the symmetrical motion of one-half the simplified elastic airplane consisting of a uniform beam with a concentrated mass at its center and subjected to a concentrated sinusoidally varying gust at station η (see fig. 1) is

$$EIz'''' = -m(y)\ddot{z} - \frac{1}{2} m_F \ddot{z}\delta(y-0) - C(k)c_{l_\alpha} qc \frac{\dot{z}}{U} + \phi(k)c_{l_\alpha} qc \frac{w}{U} e^{i\omega t}\delta(y-\eta) \tag{A1}$$

Equation (A1) is a specific form of equation (5). Since the applied force is varying sinusoidally, the steady-state response also varies sinusoidally with the same frequency and thus a solution of the form $z(y,t) = z(y,\omega)e^{i\omega t}$ can be postulated. Nondimensionalizing equation (A1) according to the definitions given in the symbol list yields

$$\bar{z}'''' = \frac{k^2}{k_a^2}\left[1 + R\delta(\bar{y}-0)\right]\bar{z} - 2i \frac{k}{k_a^2} \frac{C(k)}{\kappa_w} \bar{z} + \frac{2\phi(k)}{k_a^2 \kappa_w} \frac{w}{U} \delta(\bar{y}-\bar{\eta}) \tag{A2}$$

By using the root boundary conditions $\bar{z}'(0) = \bar{z}'''(0) = 0$, the solution of equation (A2) is obtained by the Laplace transform as

$$\bar{z} = \frac{\bar{z}(0)}{2}\left[\cosh a\bar{y} + \cos a\bar{y} - \frac{\lambda}{a^3}(\sinh a\bar{y} - \sin a\bar{y})\right] +$$

$$\frac{\bar{z}''(0)}{2a^2}(\cosh a\bar{y} - \cos a\bar{y}) + \frac{\phi(k)}{a^3 k_a^2 \kappa_w} \frac{w}{U}\left[\sinh a(\bar{y} - \bar{\eta}) -\right.$$

$$\left.\sin a(\bar{y} - \bar{\eta})\right] f(\bar{y}-\bar{\eta}) \tag{A3}$$

where

$$a = \sqrt[4]{\frac{k^2}{k_a^2} + \frac{2kG(k)}{k_a^2 \kappa_w} - \frac{2ikF(k)}{k_a^2 \kappa_w}} = g - ih$$

$$\lambda = -\frac{k^2}{k_a^2} R$$

when the second and third derivatives of equation (A3) are taken and the tip boundary conditions, $\bar{z}''(1) = \bar{z}'''(1) = 0$ are used, the unknowns $\bar{z}(0)$ and $\bar{z}''(0)$ are determined. Substituting these root conditions into equation (A3) and taking the second derivative yield

$$\bar{z}'' = \frac{\phi(k)}{ak_a^2 \kappa_w} \frac{w}{U} \left\{ \frac{1}{D} \left[\cosh a(1 - \bar{\eta}) + \cos a(1 - \bar{\eta}) \right] \left[C_1 \left(a^2 F_1 - \frac{\lambda}{a} F_2 \right) - F_3 \left(a^2 C_2 - \frac{\lambda}{a} C_3 \right) \right] - \frac{1}{D} \left[\sinh a(1 - \bar{\eta}) + \sin a(1 - \bar{\eta}) \right] \left[C_4 \left(a^2 F_1 - \frac{\lambda}{a} F_2 \right) - F_3 \left(a^2 C_3 - \frac{\lambda}{a} C_1 \right) \right] + \left[\sinh a(\bar{y} - \bar{\eta}) + \sin a(\bar{y} - \bar{\eta}) \right] 1(\bar{y} - \bar{\eta}) \right\} \qquad (A4)$$

where

$$C_1 = \cosh a + \cos a$$

$$C_2 = \cosh a - \cos a$$

$$C_3 = \sinh a + \sin a$$

$$C_4 = \sinh a - \sin a$$

$$F_1 = \cosh a\bar{y} - \cos a\bar{y}$$

$$F_2 = \sinh a\bar{y} + \sin a\bar{y}$$

$$F_3 = \cosh a\bar{y} + \cos a\bar{y}$$

$$D = 2\left[\lambda(1 + \cosh a \cos a) - a^3(\sinh a \cos a + \sin a \cosh a) \right]$$

Since $a = g - ih$ is a complex number, further manipulations are required to put the expression for $\bar{z}''$ into a form suitable for computation. The final form of $\bar{z}''$ is

$$\bar{z}''(k,\bar{\eta}) = H_{z''},_c\left[\tilde{H}_R(k,\bar{\eta}) + i\tilde{H}_I(k,\bar{\eta})\right] \tag{A5}$$

where

$$H_{z''},_c = \frac{\frac{w}{U}\,\phi(k)}{2\left(Q_1^2 + Q_2^2\right)k_a^2\kappa_w}$$

$$\tilde{H}_R(k,\bar{\eta}) = Q_9\hat{P}_{57} + Q_{10}\hat{P}_{68} - Q_{11}\hat{P}_{13} - Q_{12}\hat{P}_{\overline{24}} + A_3\left(g\grave{P}_{57} + h\grave{P}_{68}\right)I(\alpha)$$

$$\tilde{H}_I(k,\eta) = Q_{10}\hat{P}_{57} - Q_9\hat{P}_{68} - Q_{12}\hat{P}_{13} + Q_{11}\hat{P}_{\overline{24}} + A_3\left(g\grave{P}_{57} - h\grave{P}_{68}\right)I(\alpha)$$

and

$$Q_9 = Q_1Q_5 + Q_2Q_6$$

$$Q_{10} = Q_2Q_5 - Q_1Q_6$$

$$Q_{11} = Q_1Q_7 + Q_2Q_8$$

$$Q_{12} = Q_2Q_7 - Q_1Q_8$$

$$Q_5 = d_7\bar{P}_{\overline{13}} - d_8\bar{P}_{24} + d_9\bar{P}_{57} - d_{10}\bar{P}_{68} + d_{11}\bar{P}_{13} - d_{12}\bar{P}_{\overline{24}}$$

$$Q_6 = d_7\bar{P}_{24} + d_8\bar{P}_{\overline{13}} + d_9\bar{P}_{68} + d_{10}\bar{P}_{57} + d_{11}\bar{P}_{\overline{24}} + d_{12}\bar{P}_{13}$$

$$Q_7 = d_1\bar{P}_{\overline{13}} - d_2\bar{P}_{24} + d_3\bar{P}_{57} - d_4\bar{P}_{68} + d_5\bar{P}_{13} - d_6\bar{P}_{\overline{24}}$$

$$Q_8 = d_1\bar{P}_{24} + d_2\bar{P}_{\overline{13}} + d_3\bar{P}_{68} + d_4\bar{P}_{57} + d_5\bar{P}_{\overline{24}} + d_6\bar{P}_{13}$$

$$d_1 = -P_{13}\left(g^2 - h^2\right) + 2ghP_{\overline{24}}$$

$$d_2 = -P_{\overline{24}}\left(g^2 - h^2\right) - 2ghP_{13}$$

$$d_3 = \left(\frac{\lambda}{g^2 + h^2}\right)\left(gP_{13} + hP_{\overline{24}}\right)$$

$$d_4 = \left(\frac{\lambda}{g^2 + h^2}\right)\left(gP_{\overline{24}} - hP_{13}\right)$$

$$d_5 = P_{\overline{13}}\left(g^2 - h^2\right) - 2ghP_{24} - \left(\frac{\lambda}{g^2 + h^2}\right)\left(gP_{57} + hP_{68}\right)$$

$$d_6 = P_{24}\left(g^2 - h^2\right) + 2ghP_{\overline{13}} - \left(\frac{\lambda}{g^2 + h^2}\right)\left(gP_{68} - hP_{57}\right)$$

$$d_7 = -P_{\overline{57}}\left(g^2 - h^2\right) + 2ghP_{\overline{68}}$$

$$d_8 = -P_{\overline{68}}\left(g^2 - h^2\right) - 2ghP_{\overline{57}}$$

$$d_9 = \left(\frac{\lambda}{g^2 + h^2}\right)\left(gP_{\overline{57}} + hP_{\overline{68}}\right)$$

$$d_{10} = \left(\frac{\lambda}{g^2 + h^2}\right)\left(gP_{\overline{68}} - hP_{\overline{57}}\right)$$

$$d_{11} = P_{57}\left(g^2 - h^2\right) - 2ghP_{68} - d_3$$

$$d_{12} = P_{68}\left(g^2 - h^2\right) + 2ghP_{57} - d_4$$

$$A_3 = \frac{2\left(Q_1^2 + Q_2^2\right)}{g^2 + h^2}$$

$$Q_1 = \lambda q_1 - g\left(g^2 - 3h^2\right)q_2 + h\left(h^2 - 3g^2\right)q_3$$

$$Q_2 = \lambda q_4 + g\left(g^2 - 3h^2\right)q_3 + h\left(h^2 - 3g^2\right)q_2$$

$$q_1 = 1 + P_1P_3 + P_2P_4$$

$$q_2 = P_3P_5 + P_4P_6 + P_1P_7 - P_2P_8$$

$$q_3 = P_4P_5 - P_3P_6 - P_2P_7 - P_1P_8$$

$$q_4 = P_2P_3 - P_1P_4$$

$P_1 = \cosh g \cos h$ $\quad \bar{P}_1 = \cosh g\bar{y} \cos h\bar{y}$ $\quad \hat{P}_1 = \cosh g\gamma \cos h\gamma$ $\quad \grave{P}_1 = \cosh g\alpha \cos h\alpha$

$P_2 = \sinh g \sin h$ $\quad \bar{P}_2 = \sinh g\bar{y} \sin h\bar{y}$ $\quad \hat{P}_2 = \sinh g\gamma \sin h\gamma$ $\quad \grave{P}_2 = \sinh g\alpha \sin h\alpha$

$P_3 = \cos g \cosh h$ $\quad \bar{P}_3 = \cos g\bar{y} \cosh h\bar{y}$ $\quad \hat{P}_3 = \cos g\gamma \cosh h\gamma$ $\quad \grave{P}_3 = \cos g\alpha \cosh h\alpha$

$P_4 = \sin g \sinh h$ $\quad \bar{P}_4 = \sin g\bar{y} \sinh h\bar{y}$ $\quad \hat{P}_4 = \sin g\gamma \sinh h\gamma$ $\quad \grave{P}_4 = \sin g\alpha \sinh h\alpha$

$P_5 = \sinh g \cos h$ $\quad \bar{P}_5 = \sinh g\bar{y} \cos h\bar{y}$ $\quad \hat{P}_5 = \sinh g\gamma \cos h\gamma$ $\quad \grave{P}_5 = \sinh g\alpha \cos h\alpha$

$P_6 = \cosh g \sin h$ $\quad \bar{P}_6 = \cosh g\bar{y} \sin h\bar{y}$ $\quad \hat{P}_6 = \cosh g\gamma \sin h\gamma$ $\quad \grave{P}_6 = \cosh g\alpha \sin h\alpha$

$P_7 = \sin g \cosh h$ $\quad \bar{P}_7 = \sin g\bar{y} \cosh h\bar{y}$ $\quad \hat{P}_7 = \sin g\gamma \cosh h\gamma$ $\quad \grave{P}_7 = \sin g\alpha \cosh h\alpha$

$P_8 = \cos g \sinh h$ $\quad \bar{P}_8 = \cos g\bar{y} \sinh h\bar{y}$ $\quad \hat{P}_8 = \cos g\gamma \sinh h\gamma$ $\quad \grave{P}_8 = \cos g\alpha \sinh h\alpha$

$$P_{mn} = P_m + P_n$$

$$P_{\overline{mn}} = P_m - P_n$$

$$\gamma = 1 - \bar{\eta}$$

$$\alpha = \bar{y} - \bar{\eta}$$

The bending-moment response is obtained from

$$M_B = EIz'' = \frac{EI\left(\frac{c}{2}\right)}{\left(\frac{b}{2}\right)^2}\,\bar{z}'' \tag{A6}$$

Nondimensionalizing equation (A6) by the bending-moment response due to a sharp-edge gust yields

$$\frac{M_B}{M_{B,s}} = \frac{\phi(k)}{4\left(Q_1^2 + Q_2^2\right)\bar{y}_{cp}}\left[\tilde{H}_R(k,\bar{\eta}) + i\tilde{H}_I(k,\bar{\eta})\right]$$

$$= H_R(k,\bar{\eta}) + iH_I(k,\bar{\eta}) \tag{A7}$$

The bending-moment transfer-function response to a one-dimensional gust field may be obtained from the two-dimensional transfer function as follows:

$$H(k) = \int_0^1 H(k,\bar{\eta})\,d\bar{\eta} \tag{A8}$$

Integrating equation (A8) yields

$$H(k) = H_R(k) + iH_I(k) \tag{A9}$$

where

$$H_R(k) = \left(\frac{1}{g^2 + h^2}\right)\left[Q_9\acute{P}_{57} + Q_{10}\acute{P}_{68} - Q_{11}\acute{P}_{13} - Q_{12}\acute{P}_{\overline{24}} + A_3\left(g\grave{P}_{57} + h\grave{P}_{68}\right)\right]\left[\frac{\phi(k)}{4\left(Q_1^2 + Q_2^2\right)\bar{y}_{cp}}\right]$$

$$H_I(k) = \left(\frac{1}{g^2 + h^2}\right)\left[Q_{10}\acute{P}_{57} - Q_9\acute{P}_{68} - Q_{12}\acute{P}_{13} + Q_{11}\acute{P}_{\overline{24}} + A_3\left(g\grave{P}_{57} - h\grave{P}_{68}\right)\right]\left[\frac{\phi(k)}{4\left(Q_1^2 + Q_2^2\right)\bar{y}_{cp}}\right]$$

and

$$\acute{P}_{13} = gP_{57} + hP_{68}$$

$$\acute{P}_{\overline{24}} = gP_{68} - hP_{57}$$

$$\acute{P}_{57} = gP_{\overline{13}} + hP_{24}$$

$$\acute{P}_{68} = gP_{24} - hP_{\overline{13}}$$

$$\grave{P}_{57} = g\bar{P}_{\overline{13}} + h\bar{P}_{24}$$

$$\grave{P}_{68} = g\bar{P}_{24} - h\bar{P}_{\overline{13}}$$

All other terms are as defined after equation (A5) for the two-dimensional case.

APPENDIX B

MODAL ANALYSES FOR SIMPLIFIED MODEL SUBJECTED TO SYMMETRICAL PART OF RANDOM-GUST DISTURBANCES

In this appendix, solutions of the differential equations defining the symmetrical motion of the simplified model illustrated in figure 1 are obtained by two modal techniques, namely, the mode-displacement method and the force-summation method (ref. 3). Within the framework of these two methods, solutions are obtained by the Rayleigh-Ritz procedure based on an exact free-free bending mode, and, in addition, for the force-summation method, on an approximate parabolic mode.

Displacement Analysis

The determination of modal deflections is a common initial step in both the mode-displacement and the force-summation methods. The deflection expressions are a function of mode shape and thus give different results depending on whether exact- or approximate-mode shapes are employed.

The Rayleigh-Ritz equations defining the displacement in the assumed modes of an unrestrained elastic airplane subjected to an arbitrary external loading are given in reference 3. For the simplified airplane of the present study restricted to vertical rigid-body displacements and deflection in an assumed fundamental free-free symmetrical bending mode, these equations can be written in the terminology of the present report as

$$z_0\omega^2 \int_{-b/2}^{b/2} m_t(y)\,dy = C_{L_\alpha}\bar{c}q\,\frac{C(k)}{U}\,i\omega \int_{-b/2}^{b/2}\left[z_0 + z_1\xi_1(y)\right]dy - C_{L_\alpha}\bar{c}q\,\frac{\phi(k)}{U}\int_{-b/2}^{b/2} w\,dy \tag{B1}$$

$$z_1\omega^2 \int_{-b/2}^{b/2} m_t(y)\left[\xi_1(y)\right]^2 dy - z_1 \int_{-b/2}^{b/2} EI\left[\xi_1''(y)\right]^2 dy = C_{L_\alpha}\bar{c}q\,\frac{C(k)}{U}\,i\omega \int_{-b/2}^{b/2}\left\{z_0\left[\xi_1(y)\right] + z_1\left[\xi_1(y)\right]^2\right\}dy - C_{L_\alpha}\bar{c}q\,\frac{\phi(k)}{U}\int_{-b/2}^{b/2} w\xi_1(y)\,dy \tag{B2}$$

where

z_0 generalized coordinate for rigid-body translation

z_1 generalized coordinate for first free-free wing bending mode

w symmetrical part of complex amplitude of gust velocity

In writing these equations, the vertical displacement at any point on the wing was expanded in terms of the rigid-body vertical-motion mode and some mode $\xi_1(y)$, representative of the fundamental free-free mode of the simplified airplane, as

$$z = z_0 + z_1\xi_1(y) \tag{B3}$$

It was further assumed that the mode $\xi_1(y)$, whether exact or approximate, satisfies the orthogonality relation with the rigid-body mode, or that

$$\int_{-b/2}^{b/2} m_t(y)\xi_1(y)dy = 0$$

If the second term of equation (B2) is multiplied and divided by the expression $\int_{-b/2}^{b/2} m_t(y)\left[\xi_1(y)\right]^2dy$, it can be written as

$$z_1\left\{\frac{\int_{-b/2}^{b/2} EI\left[\xi_1''(y)\right]^2dy}{\int_{-b/2}^{b/2} m_t(y)\left[\xi_1(y)\right]^2dy}\right\}\int_{-b/2}^{b/2} m_t(y)\left[\xi_1(y)\right]^2dy$$

If the square of the approximate Rayleigh frequency ω_{Ra} is substituted for the term in braces, this expression becomes

$$z_1\omega_{Ra}^2\int_0^{b/2} m_t(y)\left[\xi_1(y)\right]^2dy$$

Using this expression and nondimensionalizing equations (B1) and (B2) give

$$\frac{1}{\lambda_1}\bar{z}_0 = \frac{2iC(k)}{\kappa_w k}\left(\bar{z}_0 + K_4\bar{z}_1\right) - \frac{\phi(k)}{\kappa_w k^2 U} L_g \tag{B4}$$

$$M_1\bar{z}_1\left(1 - \frac{k^2}{k_{Ra}^2}\right) = -\frac{4ikC(k)}{\kappa_w k_{Ra}^2}\left(K_4\bar{z}_0 + K_3\bar{z}_1\right) + \frac{2\phi(k)}{\kappa_w k_{Ra}^2 U} L_{g,1} \tag{B5}$$

where

$$\lambda_1 = 1 - \mu$$

$$K_3 = \frac{1}{2}\int_{-1}^{1}\left[\xi_1(\bar{y})\right]^2 d\bar{y}$$

$$K_4 = \frac{1}{2}\int_{-1}^{1}\xi_1(\bar{y})d\bar{y}$$

$$k_{Ra} = \frac{\omega_{Ra}\bar{c}}{2U}$$

$$L_g = \int_{-1}^{1} w\, d\bar{y}$$

$$L_{g,1} = \int_{-1}^{1} w\xi_1(\bar{y})d\bar{y}$$

$$M_1 = \int_{-1}^{1}\bar{m}(\bar{y})\left[\xi_1(\bar{y})\right]^2 d\bar{y}$$

$$\bar{m}(\bar{y}) = \frac{m_t(\bar{y})}{m_t(0)}$$

Solving equations (B4) and (B5) simultaneously for $\bar{z}_0$ and $\bar{z}_1$ gives

$$\bar{z}_0 = \frac{\phi(k)}{U\kappa_w k_{Ra}^2\Delta}\left(4iK_4\left[\frac{kC(k)}{\kappa_w k_{Ra}^2}\right]L_{g,1} - \left\{4iK_3\left[\frac{kC(k)}{\kappa_w k_{Ra}^2}\right] - M_1\left(1 - \frac{k^2}{k_{Ra}^2}\right)\right\}L_g\right) \tag{B6}$$

$$\bar{z}_1 = \frac{\phi(k)}{U\kappa_w k_{Ra}{}^2\Delta}\left(4iK_4\left[\frac{kC(k)}{\kappa_w k_{Ra}{}^2}\right]L_g + 2\left\{\frac{1}{\lambda_1}\frac{k^2}{k_{Ra}{}^2} - 2i\left[\frac{kC(k)}{\kappa_w k_{Ra}{}^2}\right]\right\}L_{g,1}\right) \quad (B7)$$

where

$$\Delta = 8\left(K_3 - K_4{}^2\right)\left[\frac{kC(k)}{\kappa_w k_{Ra}{}^2}\right]^2 - 2i\left[M_1\left(1 - \frac{k^2}{k_{Ra}{}^2}\right) - 2\frac{K_3 k^2}{\lambda_1 k_{Ra}{}^2}\right]\left[\frac{kC(k)}{\kappa_w k_{Ra}{}^2}\right] + \frac{M_1 k^2}{\lambda_1 k_{Ra}{}^2}\left(1 - \frac{k^2}{k_{Ra}{}^2}\right) \quad (B8)$$

If an exact free-free bending mode for the system is used rather than an approximate shape, the Rayleigh frequency ω_{Ra} is identical to the exact fundamental-bending-mode frequency for the system ω_1 and, thus, $k_1 = k_{Ra}$. Where the exact frequency is known but the exact mode is unknown, an increase in accuracy can normally be obtained by using the exact frequency in place of ω_{Ra}. This procedure is referred to as a modified Rayleigh-Ritz approach in the present report.

Bending Moments Due to a Two-Dimensional Gust Distribution

Mode-displacement method.- In the mode-displacement method, the bending moment is defined by simple beam theory as

$$M_B = EI\left(y_1\right)\sum_{n=0}^{r-1} z_n \xi_n{}''\left(y_1\right) \quad (B9)$$

In the present study, EI is a constant and $\xi_0{}''\left(y_1\right)$ is equal to zero; thus,

$$M_B = EIz_1\xi_1{}''\left(y_1\right) \quad (B10a)$$

or

$$M_B = \frac{EI\left(\frac{c}{2}\right)}{\left(\frac{b}{2}\right)^2} z_1\xi_1{}''\left(y_1\right) \quad (B10b)$$

Dividing equation (B10b) by the bending moment due to a sharp-edge gust and substituting equation (B7) for $\bar{z}_1$ give

$$\frac{M_B}{M_{B,s}} = H_0 L_g + H_1 L_{g,1} \tag{B11a}$$

where

$$\left.\begin{aligned} H_0 &= 2iK_4 \frac{kC(k)}{\kappa_w k_{Ra}^2}\left[\frac{k_1^2 \xi_1''(y_1)\phi(k)}{k_{Ra}^2 \bar{y}_{cp}\,\Delta}\right] \\ H_1 &= \left[\frac{k^2}{\lambda_1 k_{Ra}^2} - 2i\,\frac{kC(k)}{\kappa_w k_{Ra}^2}\right]\left[\frac{k_1^2 \xi_1''(y_1)\phi(k)}{k_{Ra}^2 \bar{y}_{cp}\,\Delta}\right] \end{aligned}\right\} \tag{B11b}$$

If the procedure described in reference 4 is used, the spectrum of the output bending-moment ratio is written as

$$\frac{\Phi_{MB}(k)}{(M_{B,s})^2} = |H_0|^2 \Phi_{w_{00}}(k) + |H_1|^2 \Phi_{w_{11}}(k) + 2\mathrm{Re}\left(H_0 H_1^*\right)\Phi_{w_{01}}(k) \tag{B12}$$

where

$$\Phi_{w_{mn}}(k) = \int_0^2 \Phi_w(k,\bar{\theta})\,d\bar{\theta} \int_{-1}^{1-\bar{\theta}} \gamma_m(\bar{\eta})\gamma_n(\bar{\eta}+\bar{\theta})\,d\bar{\eta} \tag{B13}$$

and

$$\gamma_0(\bar{\eta}) = 1$$

$$\gamma_1(\bar{\eta}) = \xi_1(\bar{\eta})$$

Equation (B13) is a slightly modified version of equation (11).

Equation (B13) can be used with either an exact bending mode or an approximate mode which satisfies the orthogonality condition with the rigid-body mode. Unless the second derivative of the approximate mode is a very good approximation of the second derivative of the exact mode, however, the bending-moment result cannot be expected to be very accurate.

Force-summation method.- In the force-summation method, the inertia and the aerodynamic loading due to wing motions in the various modes are

integrated together with the external gust loading to obtain the desired bending moment as follows:

$$M_B = \int_{y_1}^{b/2} \left(l_i + l_m + l_g\right)\left(y - y_1\right)dy \tag{B14}$$

where l_i and l_m are the inertia and aerodynamic loadings associated with the deflections of the rigid body and fundamental modes and l_g is the symmetrical part of the loading due directly to the gusts and they are defined by the following equations:

$$l_i = m_t(y)\omega^2\left(z_0 + z_1\xi_1(y)\right)$$

$$l_m = -\frac{c l_\alpha cq}{U} C(k)\left(z_0 + z_1\xi_1(y)\right) i\omega$$

$$l_g = \frac{c l_\alpha cq}{U} \phi(k) w$$

Substituting the previously derived expressions for $\bar{z}_0$ and $\bar{z}_1$ (eqs. (B6) and (B7)) into equation (B14) and manipulating the result gives, after dividing by the bending moment due to the sharp-edge gust,

$$\frac{M_B}{M_{B,s}} = H_0 L_g + H_1 L_{g,1} + H_2 L_{g,2} \tag{B15a}$$

where

$$\left.\begin{aligned} H_0 &= \left(T_1 + iT_2\right)\left(T_3 + iT_4\right)\left[\frac{\phi(k)}{\bar{y}_{cp}\,\Delta}\right] \\ H_1 &= \left(T_1 + iT_2\right)\left(T_5 + iT_6\right)\left[\frac{\phi(k)}{\bar{y}_{cp}\,\Delta}\right] \\ H_2 &= \Delta = T_7 + iT_8 \\ L_{g,2} &= \int_{\bar{y}_1}^{1} \left(\bar{y} - \bar{y}_1\right) w \, d\bar{y} \end{aligned}\right\} \tag{B15b}$$

and

$$T_1 = \frac{1}{k_{Ra}^2}\left(k^2 + \hat{G}\right)$$

$$T_2 = -\frac{\hat{F}}{k_{Ra}^2}$$

$$T_3 = \frac{\hat{G}}{k_{Ra}^2}\left[K_3\bar{y}_{cp} - K_4\left(I_2 - I_1\right)\right] - \lambda_2\bar{y}_{cp}\left(1 - \frac{k^2}{k_{Ra}^2}\right)$$

$$T_4 = -\frac{\hat{F}}{k_{Ra}^2}\left[K_3\bar{y}_{cp} - K_4\left(I_2 - I_1\right)\right]$$

$$T_5 = -\hat{G}K_4\frac{\bar{y}_{cp}}{k_{Ra}^2} + \left(\frac{1}{\lambda_1}\frac{k^2}{k_{Ra}^2} + \frac{\hat{G}}{k_{Ra}^2}\right)\left(I_2 - I_1\right)$$

$$T_6 = \hat{F}K_4\frac{\bar{y}_{cp}}{k_{Ra}^2} - \frac{\hat{F}}{k_{Ra}^2}\left(I_2 - I_1\right)$$

$$T_7 = \frac{2}{k_{Ra}^4}\left(K_4^2 - K_3\right)\left(\hat{G}^2 - \hat{F}^2\right) + 2\left[\lambda_2\left(1 - \frac{k^2}{k_{Ra}^2}\right) - \frac{K_3}{\lambda_1}\frac{k^2}{k_{Ra}^2}\right]\frac{\hat{G}}{k_{Ra}^2} + \frac{2\lambda_2 k^2}{\lambda_1 k_{Ra}^2}\left(1 - \frac{k^2}{k_{Ra}^2}\right)$$

$$T_8 = -\frac{4}{k_{Ra}^4}\left(K_4^2 - K_3\right)\hat{G}\hat{F} - 2\left[\lambda_2\left(1 - \frac{k^2}{k_{Ra}^2}\right) - \frac{K_1}{\lambda_1}\frac{k^2}{k_{Ra}^2}\right]\frac{\hat{F}}{k_{Ra}^2}$$

$$\hat{G} = \frac{2k}{\kappa_w}\left[G(k) + \frac{k}{2}\right]$$

$$\hat{F} = \frac{2k}{\kappa_w}F(k)$$

$$I_1 = \bar{y}_1\int_{\bar{y}_1}^{1}\xi_1(\bar{y})\,d\bar{y}$$

$$I_2 = \int_{\bar{y}_1}^{1} \bar{y}\xi_1(\bar{y})d\bar{y}$$

$$\lambda_2 = K_3 + R\left[\xi_1(0)\right]^2$$

When the procedure given in reference 4 is used, the spectrum of output bending-moment ratio is written as,

$$\frac{\Phi_{MB}(k)}{(M_{B,s})^2} = |H_0|^2\Phi_{w_{00}}(k) + |H_1|^2\Phi_{w_{11}}(k) + |H_2|^2\Phi_{w_{22}}(k) + 2Re(H_0H_1^*)\Phi_{w_{01}}(k) + 2Re(H_0H_2^*)\Phi_{w_{02}}(k) + 2Re(H_1H_2^*)\Phi_{w_{12}}(k) \quad (B16)$$

where the functions $\Phi_{w_{mn}}(k)$ are as defined in the preceding section and $\gamma_2(\bar{\eta}) = \frac{1}{2}\left[(\bar{\eta} - \bar{y}_1)1(\bar{\eta}-\bar{y}_1) + (-\bar{\eta} - \bar{y}_1)1(-\bar{\eta}-\bar{y}_1)\right]$. Equation (B16) is an expanded version of equation (11) and can be used with an exact bending mode or an approximate mode which satisfies the orthogonality relation with the rigid-body mode.

Bending Moments Due to a One-Dimensional Gust Distribution

Mode-displacement method.- In the mode-displacement method for the one-dimensional gust distribution, the integrals defining L_g and $L_{g,1}$ can be evaluated exactly. These integrations yield

$$\left.\begin{aligned} L_g &= 2w \\ L_{g,1} &= 2wK_4 \end{aligned}\right\} \quad (B17)$$

Substituting equations (B17) into equation (B11) gives

$$\frac{M_B}{M_{B,s}} = \left(2H_0 + 2K_4H_1\right)w \quad (B18)$$

Then the output bending-moment spectrum becomes,

$$\frac{\Phi_{MB}(k)}{(M_{B,s})^2} = \left[|2H_0|^2 + |2K_4H_1|^2 + 8K_4Re(H_0H_1^*)\right]\Phi_w(k) \quad (B19)$$

Equations (B18) and (B19) can be simplified somewhat by combining terms, but this was not done since H_0 and H_1 for the two-dimensional case had to be determined in any event.

Force-summation method.- In the force-summation method, for the one-dimensional gust distribution, the integral expression for $L_{g,2}$ evaluated exactly yields

$$L_{g,2} = \bar{y}_{cp} w \tag{B20}$$

Substituting equations (B20) and (B17) into equation (B15) gives

$$\frac{M_B}{M_{B,s}} = w\left(2H_0 + 2K_4 H_1 + \bar{y}_{cp} H_2\right) \tag{B21}$$

The output bending-moment spectrum for the one-dimensional gust distribution can then be written as,

$$\frac{\Phi_{MB}(k)}{\left(M_{B,s}\right)^2} = \left[4\left|H_0\right|^2 + 4K_4\left|H_1\right|^2 + \bar{y}_{cp}{}^2\left|H_2\right|^2 + 8K_4 \mathrm{Re}\left(H_0 H_1{}^*\right) + 4\bar{y}_{cp}\mathrm{Re}\left(H_0 H_2{}^*\right) + 4K_4\bar{y}_{cp}\mathrm{Re}\left(H_1 H_2{}^*\right)\right]\Phi_w(k) \tag{B22}$$

APPENDIX C

MATRIX METHOD FOR SIMPLIFIED MODELS SUBJECTED TO THE SYMMETRICAL PART OF A RANDOM-GUST DISTURBANCE

The differential equation defining the symmetrical motions of one-half the simplified wing-fuselage combination treated in this paper (fig. 1) and subjected to a sinusoidal gust velocity at station η on the span is given by equation (A2) as

$$\bar{z}'''' = \frac{k^2}{{k_a}^2}\left[1 + R\delta(\bar{y}-0)\right]\bar{z} - 2i\,\frac{k}{{k_a}^2}\,\frac{C(k)}{\kappa_w}\,\bar{z} + \frac{2\phi(k)}{{k_a}^2\kappa_w}\,\frac{w}{U}\,\delta(\bar{y}-\bar{\eta}) \tag{C1}$$

Integrating equation (C1) twice by using two of the four appropriate boundary conditions; namely $\bar{z}'' = \bar{z}''' = 0$ at $\bar{y} = 1$ gives

$$\bar{z}'' = \frac{1}{{k_a}^2}\int_{\bar{y}}^{1}\int_{\bar{y}}^{1}\left\{k^2\left[1 + R\delta(\bar{y}-0)\right]\bar{z} - 2ik\,\frac{C(k)}{\kappa_w}\,\bar{z} + \frac{2\phi(k)}{\kappa_w}\,\frac{w}{U}\,\delta(\bar{y}-\bar{\eta})\right\}d\bar{y}\,d\bar{y} \tag{C2}$$

By definition

$$\bar{z} = \iint \bar{z}''\,d\bar{y}\,d\bar{y}$$

Using the boundary condition that the slope of the wing bending deflection at the fuselage center line ($\bar{y} = 0$) must be zero for symmetrical motions in this definition yields

$$\bar{z} = \bar{z}_0 + \int_0^{\bar{y}}\int_0^{\bar{y}} \bar{z}''\,d\bar{y}\,d\bar{y} \tag{C3}$$

Substituting equation (C3) into equation (C2) gives

$$\bar{z}'' = \frac{1}{{k_a}^2}\int_{\bar{y}}^{1}\int_{\bar{y}}^{1}\left(\left\{k^2\left[1 + R\delta(\bar{y}-0)\right] - 2ik\,\frac{C(k)}{\kappa_w}\right\}\left(\bar{z}_0 + \int_0^{\bar{y}}\int_0^{\bar{y}} \bar{z}''\,d\bar{y}\,d\bar{y}\right) + \frac{2\phi(k)}{\kappa_w}\,\frac{w}{U}\,\delta(\bar{y}-\bar{\eta})\right)d\bar{y}\,d\bar{y} \tag{C4}$$

Dividing the beam into $n - 1$ segments, equation (C4) can be written as an nth-order matrix equation. Designating $\left[I_1\right] = \int_{\bar{y}}^{1}$, $\left[II_1\right] = \int_{\bar{y}}^{1}\int_{\bar{y}}^{1}$, $\left[I_2\right] = \int_{0}^{\bar{y}}$, and $\left[II_2\right] = \int_{0}^{\bar{y}}\int_{0}^{\bar{y}}$ as integrating matrices for the continuous functions in equation (C4) and integrating the delta functions exactly allows equation (C4) to be written as

$$\left\{\bar{z}''\right\} = \frac{k^2}{k_a{}^2}\left[II_1\right]\left[1 - 2i\,\frac{C(k)}{k\kappa_w}\right]\left\{\left\{\bar{z}_0\right\} + \left[II_2\right]\left\{\bar{z}''\right\}\right\} + \frac{2\phi(k)}{k_a{}^2\kappa_w}\,\frac{w}{U}\left\{(\bar{\eta} - \bar{y})/(\bar{\eta}-\bar{y})\right\} \tag{C5}$$

Under the assumption of symmetrical bending deflections, the shear at the fuselage center line must be zero; thus,

$$(EIz'')'_{y=0} = 0 = \int_{0}^{b/2}\left(l_i + l_m + l_g\right)dy \tag{C6}$$

Equation (C6) can be written in matrix notation as follows:

$$0 = k^2\left[\left\lfloor I\right\rfloor\left[1 - 2i\,\frac{C(k)}{k\kappa_w}\right] + R\left\lfloor I_3\right\rfloor\right]\left\{\left\{\bar{z}_0\right\} + \left[II_2\right]\left\{\bar{z}''\right\}\right\} + \frac{2\phi(k)}{\kappa_w}\,\frac{w}{U} \tag{C7}$$

where $\left\lfloor I\right\rfloor$ is a row matrix of integrating factors for the range 0 to 1 and $\left\lfloor I_3\right\rfloor = \left\lfloor 1\ 0\ 0\ 0\ 0\right\rfloor$ for $n = 5$.

Solving equation (C7) for $\left\{\bar{z}_0\right\}$ gives

$$\left\{\bar{z}_0\right\} = \frac{1}{\kappa_1}\left\{\left[\left[I\right]\left[1 - 2i\,\frac{C(k)}{k\kappa_w}\right] + R\left[I_3\right]\right]\left[II_2\right]\left\{\bar{z}''\right\} + \frac{2\phi(k)}{k^2\kappa_w}\,\frac{w}{U}\left\{1\right\}\right\} \tag{C8}$$

where

$$\kappa_1 = -\left[\left\lfloor I\right\rfloor\left[1 - 2i\,\frac{C(k)}{k\kappa_w}\right] + R\left[I_3\right]\right]\left\{1\right\}$$

and $\left[I\right]$ and $\left[I_3\right]$ are composed of identical rows of $\left\lfloor I\right\rfloor$ and of $\left\lfloor I_3\right\rfloor$, respectively.

Substituting $\{\bar{z}_0\}$ from equation (C8) into equation (C5) yields, after rearranging terms,

$$\left[\left[1\right] - \frac{k^2}{k_a{}^2}\left[II_1\right]\left[1 - 2i\,\frac{C(k)}{k\kappa_w}\right]\left[\left[1\right] + \frac{1}{\kappa_1}\left[\left[I\right]\left[1 - 2i\,\frac{C(k)}{k\kappa_w}\right] + R\left[I_3\right]\right]\right]\left[II_2\right]\right]\{z''\} =$$

$$\frac{2\phi(k)}{\kappa_w\kappa_1 k_a{}^2}\,\frac{w}{U}\left[II_1\right]\left[1 - 2i\,\frac{C(k)}{k\kappa_w}\right]\{1\} + \frac{2\phi(k)}{k_a{}^2\kappa_w}\,\frac{w}{U}\left\{(\bar{\eta} - \bar{y})/(\bar{\eta}-\bar{y})\right\} \qquad (C9)$$

From equation (C9), $\bar{z}''$ is obtained by inverting the matrix premultiplying $\{\bar{z}''\}$ at any or all of the n stations due to a sinusoidal gust of intensity w applied at any station η on the wing. Note that η need not be at the stations into which the wing is divided; it may be anywhere on the wing. In the computations performed in the present report, only 5 stations were used but 10 equally spaced values of η were required to obtain reasonable accuracy in subsequent numerical integrations.

In the computations, the following integrating matrices from reference 6 were used:

$$\left[I\right] = \frac{0.2}{3}\begin{bmatrix} 1 & 4 & 2 & 4 & 1 \end{bmatrix}$$

$$\left[II_1\right] = \frac{(0.2)^2}{24}\begin{bmatrix} 2 & 24 & 44 & 88 & 34 \\ 0 & 2 & 21 & 60 & 25 \\ 0 & 0 & 0 & 32 & 16 \\ 0 & 0 & -1 & 6 & 7 \\ 0 & 0 & 0 & 0 & 0 \end{bmatrix}$$

$$\left[II_2\right] = \frac{(0.2)^2}{24}\begin{bmatrix} 0 & 0 & 0 & 0 & 0 \\ 7 & 6 & -1 & 0 & 0 \\ 16 & 32 & 0 & 0 & 0 \\ 25 & 60 & 21 & 2 & 0 \\ 34 & 88 & 44 & 24 & 2 \end{bmatrix}$$

The bending moment is obtained from

$$M_B = EIz'' = \frac{EI\left(\frac{c}{2}\right)}{\left(\frac{b}{2}\right)^2} \bar{z}'' \tag{C10}$$

Nondimensionalizing equation (C10) by the bending-moment response due to a sharp-edge gust yields

$$\frac{M_B}{M_{B,s}} = \frac{k_a{}^2 \kappa_w}{2\bar{y}_{cp} \frac{w}{U}} \bar{z}'' = H_R(k,\bar{\eta}) + iH_I(k,\bar{\eta}) \tag{C11}$$

The bending-moment transfer-function response for a one-dimensional gust field may be obtained by simple numerical integration over $\bar{\eta}$ of the two-dimensional transfer function; that is,

$$H(k) = \int_0^1 H(k,\bar{\eta})d\bar{\eta} \tag{C12}$$

APPENDIX D

ANALYSIS FOR SIMPLIFIED RIGID MODEL SUBJECTED TO THE SYMMETRICAL PART OF A RANDOM-GUST DISTURBANCE

In this appendix, an exact solution is made for the symmetrical response of a simplified rigid airplane to random vertical gust excitation. (See fig. 1.) The basic differential equation defining vertical motions of this system is

$$0 = l_i + l_m + l_g \tag{D1}$$

(which is a specific form of eq. (5)) where l_i is the inertia loading per unit span and l_g and l_m are, respectively, the aerodynamic loadings per unit span due directly to the symmetrical part of the gust and those due to wing vertical motions. Since the flexibility term is missing in equation (D1), it can be solved exactly for the system motions.

Displacement Analysis

Under the assumptions of the present study (see appendix B), equation (D1) can be rewritten as

$$m_t(y)\ddot{z}_0 + C_{L_\alpha} Sq \frac{C(k)}{U} \dot{z}_0 - \int_{-b/2}^{b/2} c_{l_{c_\alpha}} cq \frac{w}{U} \phi(k)dy = 0 \tag{D2}$$

If sinusoidal excitation is assumed, equation (D2) is solved directly for the rigid-body displacement. This has been done in reference 3, and in the terminology of the present analysis the equation is written in nondimensional form as

$$\bar{z}_0 = \frac{1}{k^2}\left[\frac{\phi(k)}{-\kappa + 2i\frac{C(k)}{k}}\right]\frac{1}{\bar{U}} \int_{-1}^{1} w \, d\bar{y} \tag{D3}$$

Bending-Moment Analysis

The bending moment is obtained from the following simple integration of the loadings (force-summation method):

$$M_B = \int_{y_1}^{b/2} (y - y_1)(l_i + l_m + l_g)dy \tag{D4}$$

where, for the rigid airplane,

$$l_i = \frac{c}{2} m_t(y)\omega^2 \bar{z}_0$$

$$l_m = - \frac{c l_\alpha q i\omega \frac{c^2}{2} C(k)}{U} \bar{z}_0$$

$$l_g = c l_\alpha q c \phi(k) \frac{w}{U}$$

Substituting equation (D3) into equation (D4) and dividing by the bending moment due to a sharp-edge gust results in the following expression:

$$\frac{M_B}{M_{B,s}} = H_0 L_g + H_2 L_{g,2} \tag{D5}$$

where

$$H_0 = - \frac{1}{2} \phi(k) \left\{ 1 - \frac{k\kappa\mu \left[k(\kappa + 1) + 2G(k) - 2iF(k) \right]}{\left[k(\kappa + 1) + 2G(k) \right]^2 + 4\left[F(k) \right]^2} \right\}$$

$$H_2 = \frac{\phi(k)}{\bar{y}_{cp}}$$

If the same procedure employed in the analysis for the flexible airplane is followed in the analysis for the symmetrical response of the rigid airplane, the spectrum of the output bending-moment ratio for the two-dimensional gust distribution is

$$\frac{\left[\Phi_{MB}(k) \right]_r}{(M_{B,s})^2} = |H_0|^2 \Phi_{w_{00}}(k) + |H_2|^2 \Phi_{w_{22}}(k) + 2\mathrm{Re}\left(H_0 H_2^* \right) \Phi_{w_{20}}(k) \tag{D6}$$

For the one-dimensional gust distribution - that is, w constant along the span - equation (D6) reduces to

$$\frac{\left[\Phi_{MB}(k) \right]_r}{(M_{B,s})^2} = \left| 1 + 2H_0 \right|^2 \Phi_w(k) \tag{D7}$$

An exact solution can be obtained for the output bending-moment spectrum of a rigid airplane traversing a random two-dimensional gust field with the distribution characteristics defined by equation (7). The solution, however, is highly subject to small difference difficulties, and since the functions involved have not been tabulated with a sufficient degree of accuracy, no results have been computed which may be used as a check comparison on the numerical integrations performed.

REFERENCES

1. Press, Harry, and Houbolt, John C.: Some Applications of Generalized Harmonic Analysis to Gust Loads on Airplanes. Jour. Aero. Sci., vol. 22, no. 1, Jan. 1955, pp. 17-26, 60.

2. Diederich, Franklin W.: The Response of an Airplane to Random Atmospheric Disturbances. NACA Rep. 1345, 1958. (Supersedes NACA TN 3910.)

3. Bisplinghoff, Raymond L., Ashley, Holt, and Halfman, Robert L.: Aeroelasticity. Addison-Wesley Pub. Co., Inc. (Cambridge, Mass.), c.1955.

4. Diederich, Franklin W.: The Dynamic Response of a Large Airplane to Continuous Random Atmospheric Disturbances. Jour. Aero. Sci., vol. 23, no. 10, Oct. 1956, pp. 917-930.

5. Press, Harry, and Tukey, John W.: Power Spectral Methods of Analysis and Their Application to Problems in Airplane Dynamics. Vol. IV of AGARD Flight Test Manual, Pt. IVC, Enoch J. Durbin, ed., North Atlantic Treaty Organization (Paris), pp. IVC:1 - IVC-41.

6. Benscoter, Stanley U., and Gossard, Myron L.: Matrix Methods for Calculating Cantilever-Beam Deflections. NACA TN 1827, Mar. 1947.

7. Diederich, Franklin W., and Drischler, Joseph A.: Effect of Spanwise Variations in Gust Intensity on the Lift Due to Atmospheric Turbulence. NACA TN 3920, 1957.

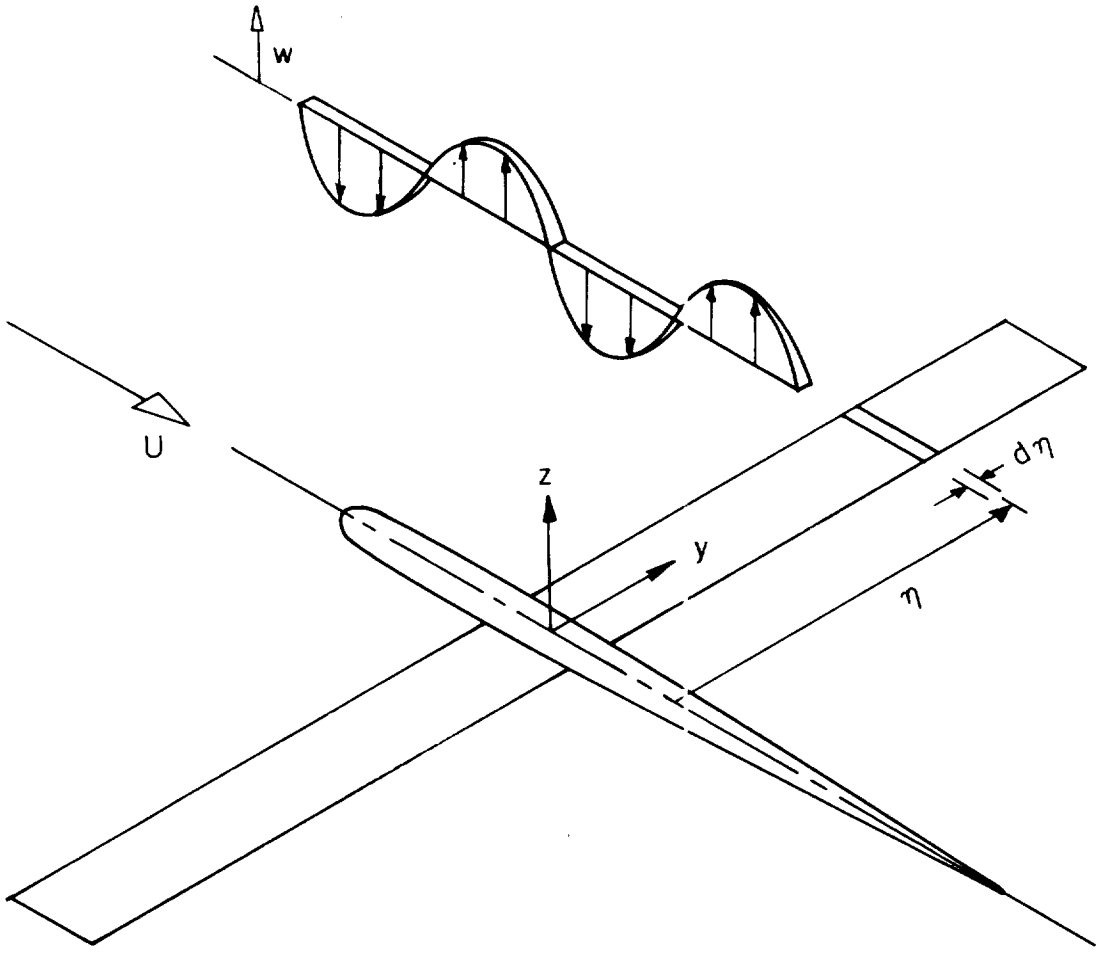

Figure 1.- Simplified airplane subjected to sinusoidal gust velocity.

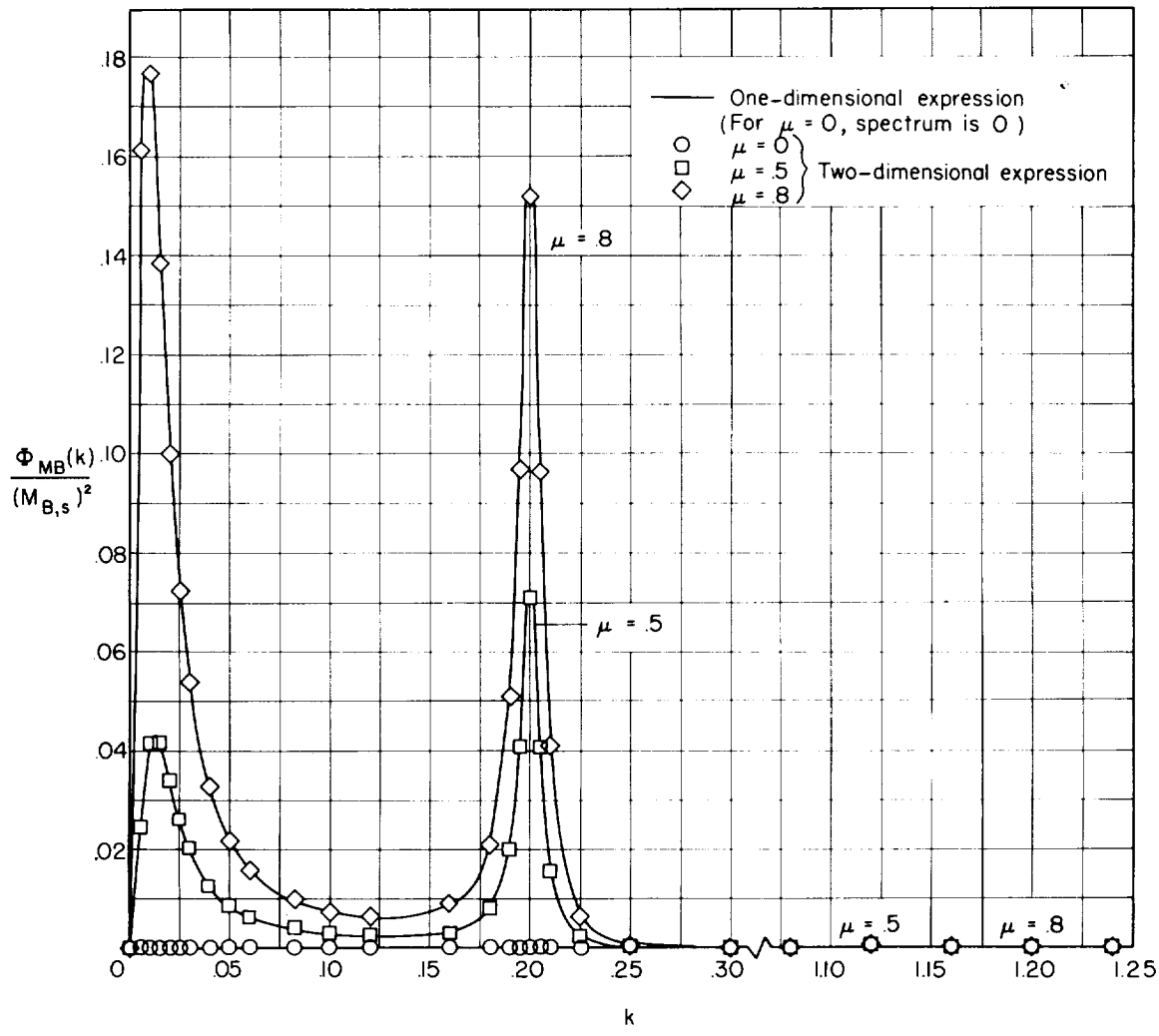

(a) $\bar{y}_1 = 0.$

Figure 2.- Output bending-moment spectra for one-dimensional gust turbulence, obtained from the one- and two-dimensional turbulence expressions.

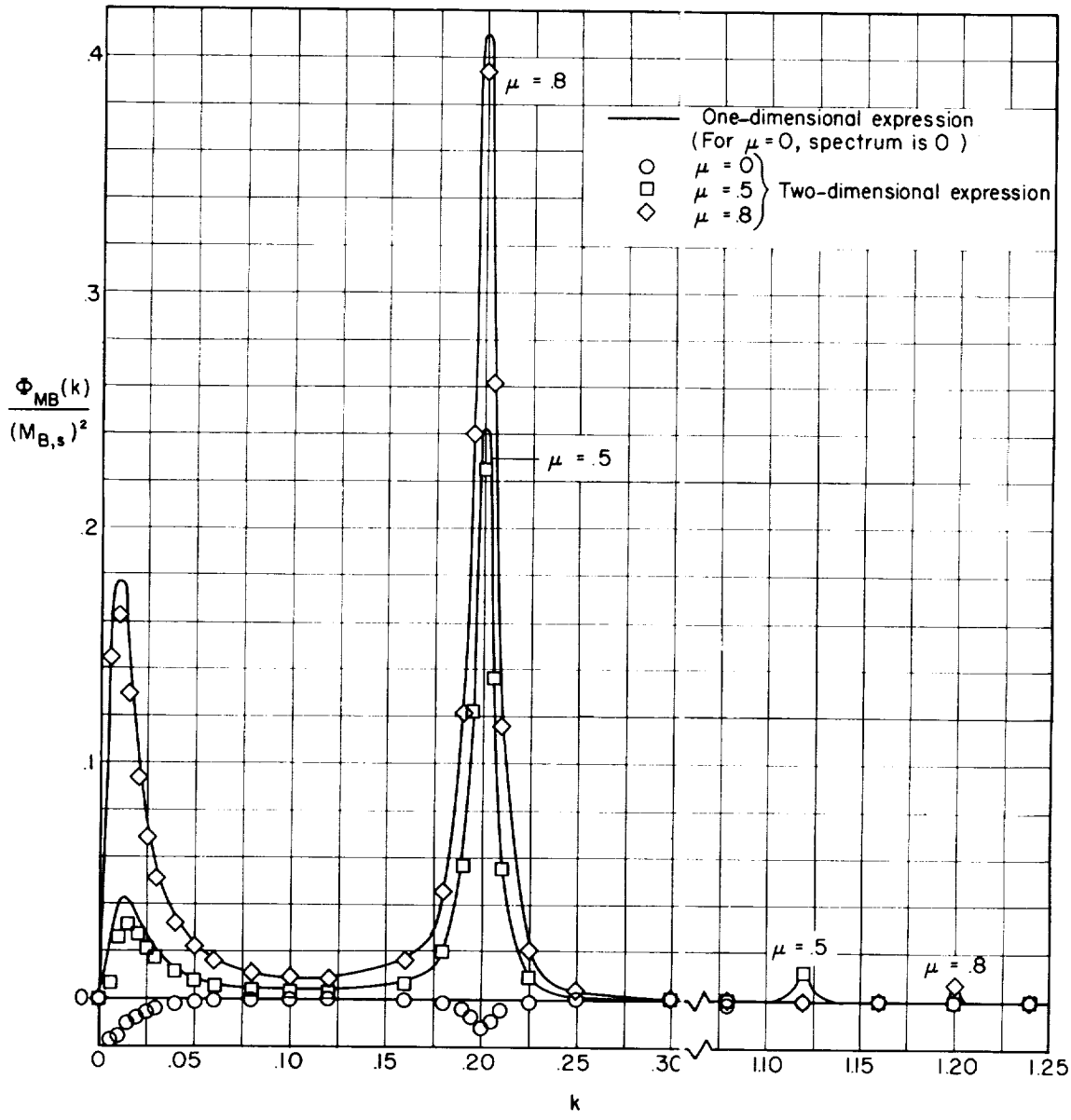

(b) $\overline{y}_1 = 0.75$.

Figure 2.- Concluded.

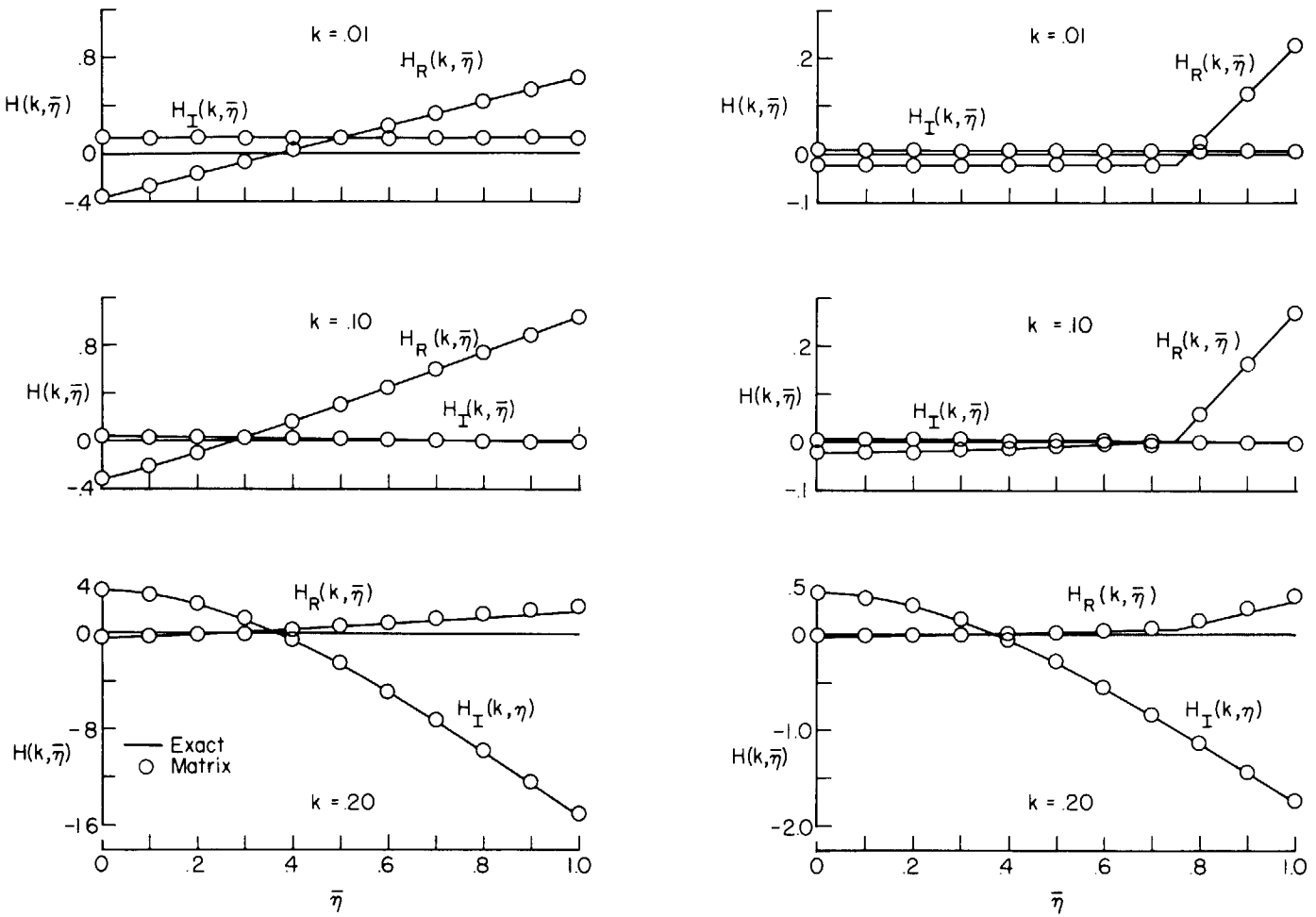

(a) $\bar{y}_1 = 0.$

(b) $\bar{y}_1 = 0.75.$

Figure 3.- Sample plots of frequency-response functions. $\mu = 0.5$.

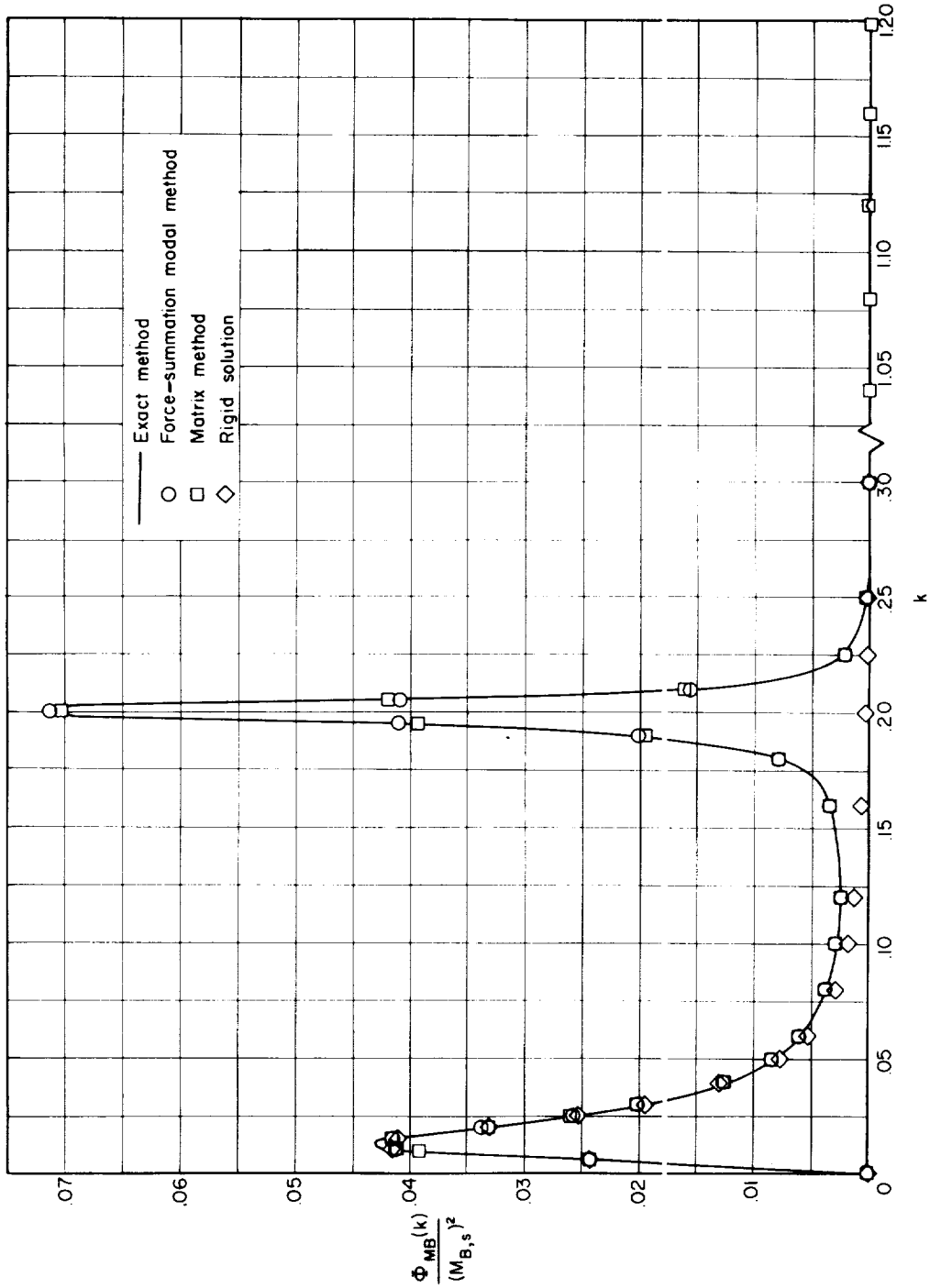

(a) Output bending-moment spectra for one-dimensional turbulence. $\mu = 0.5$; $\bar{y}_1 = 0$.

Figure 4.- Evaluation of the more accurate approximate procedures by spectra comparison.

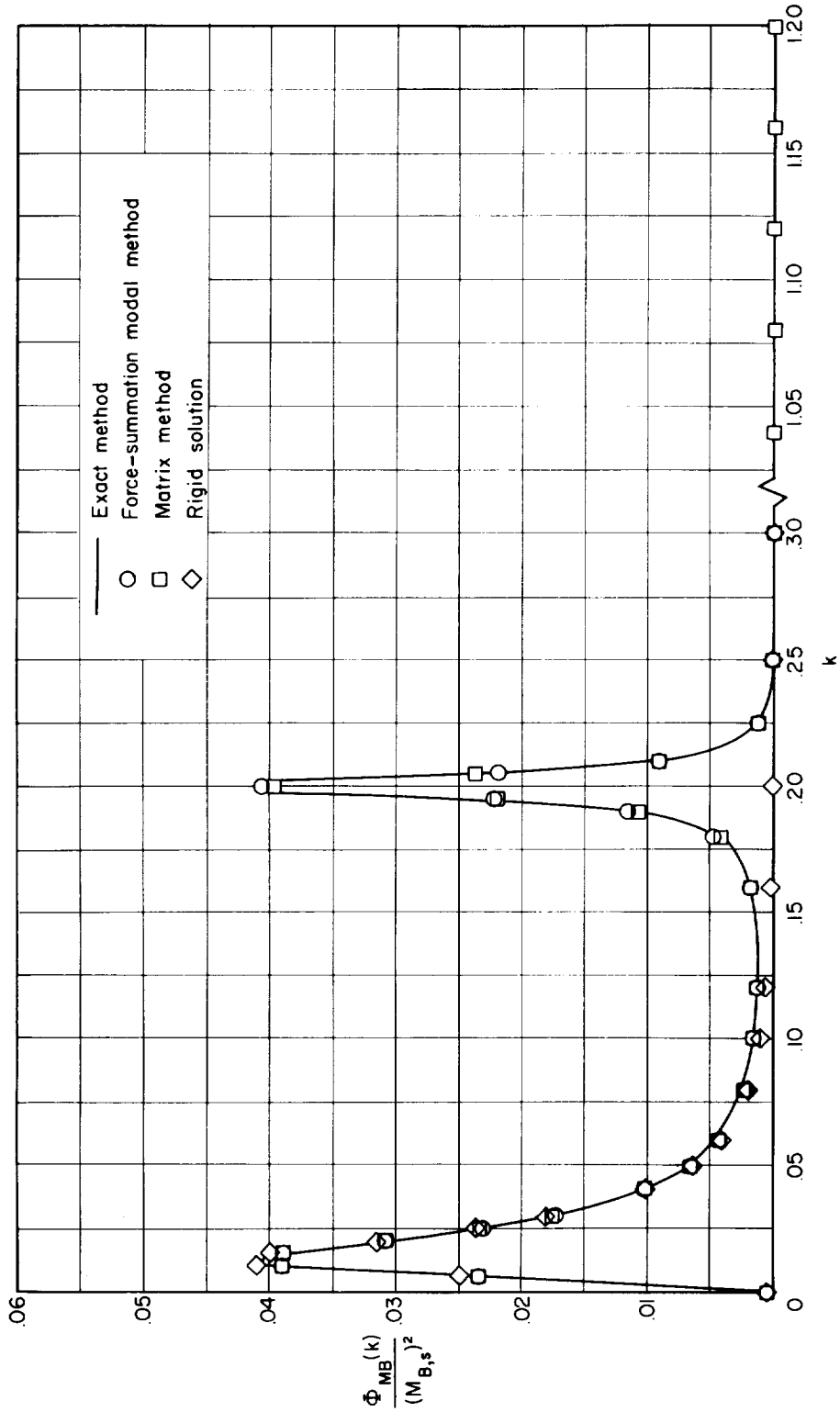

(b) Output bending-moment spectra for two-dimensional turbulence. $\mu = 0.5$; $\bar{y}_1 = 0$.

Figure 4.- Continued.

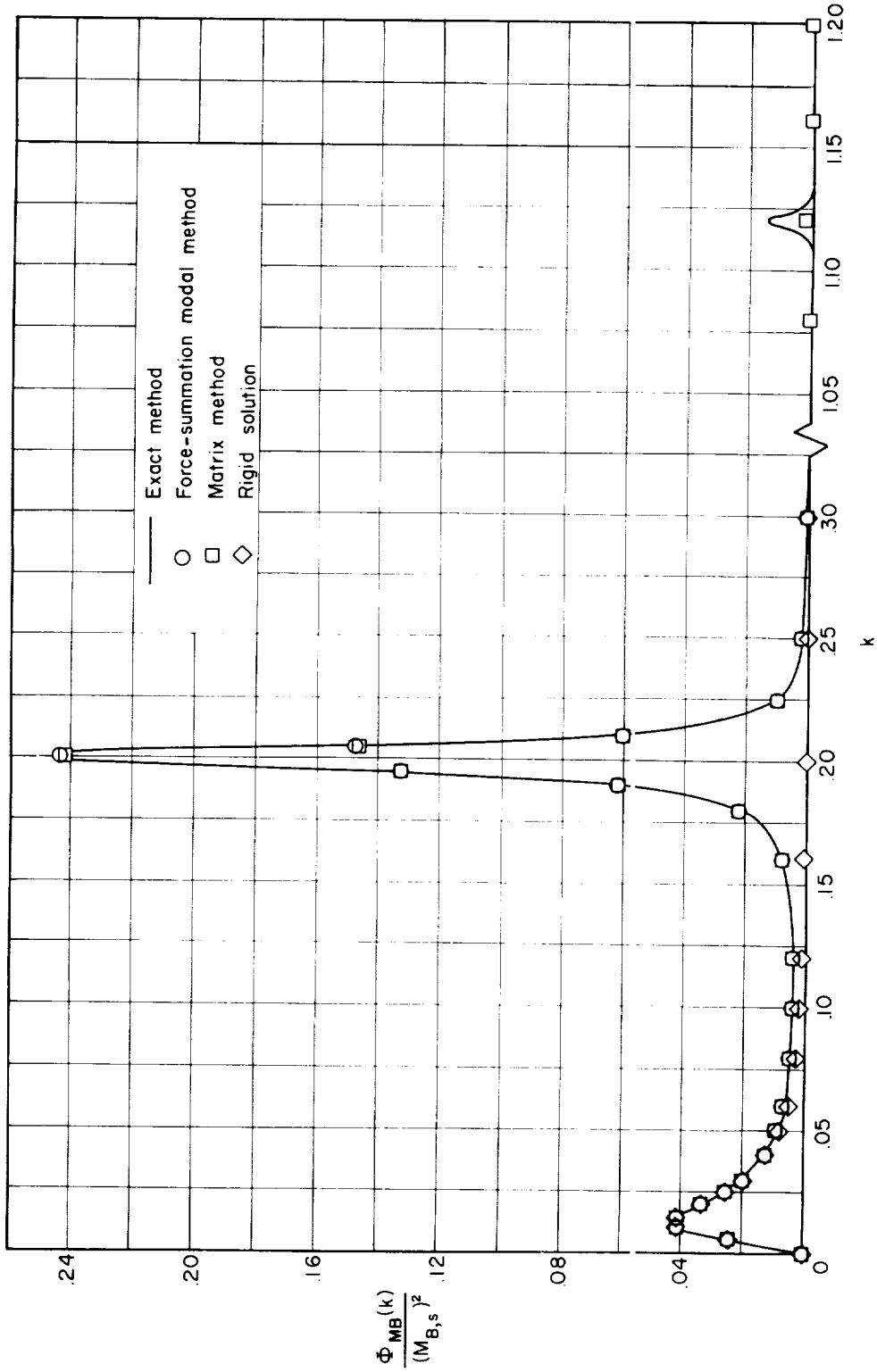

(c) Output bending-moment spectra for one-dimensional turbulence. $\mu = 0.5$; $\bar{y}_1 = 0.75$.

Figure 4.- Continued.

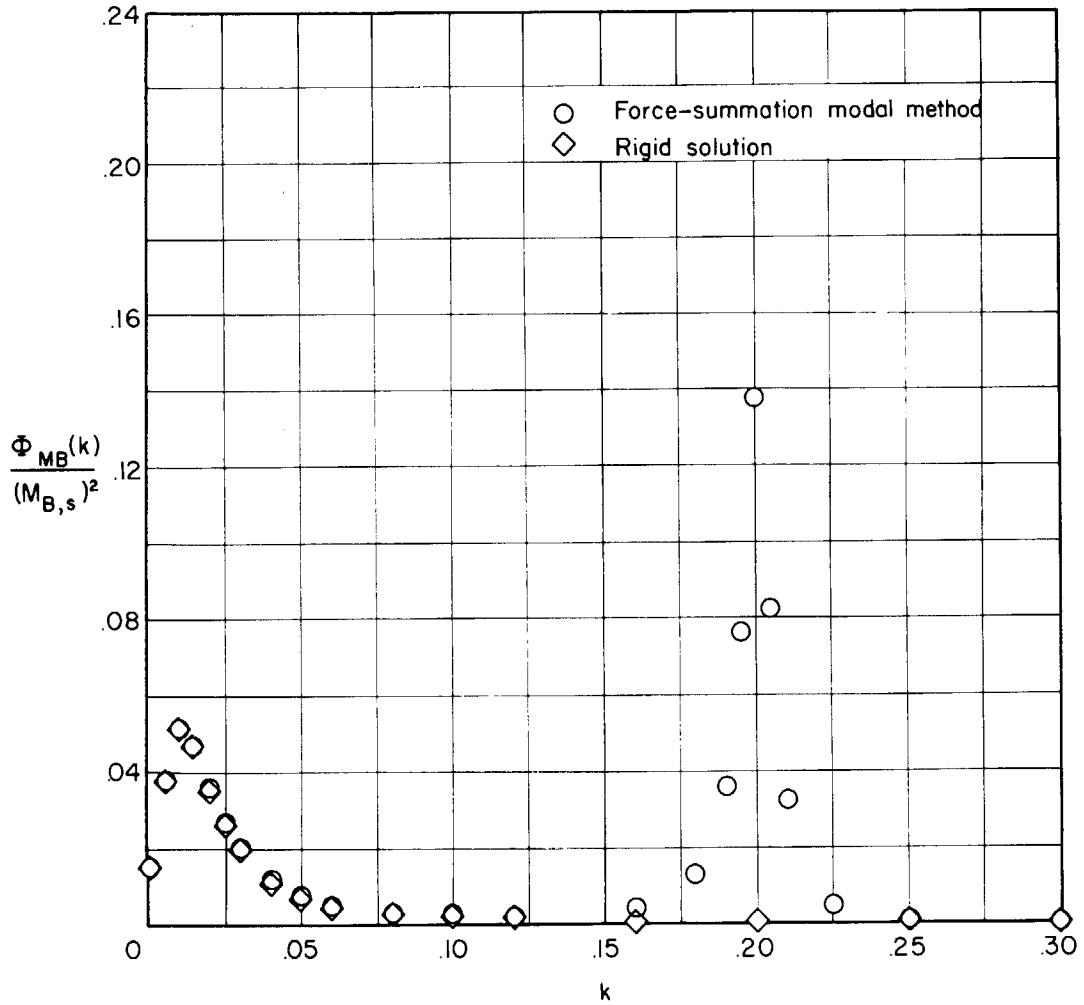

(d) Output bending-moment spectra for two-dimensional turbulence. $\mu = 0.5$; $\overline{y}_1 = 0.75$.

Figure 4.- Concluded.

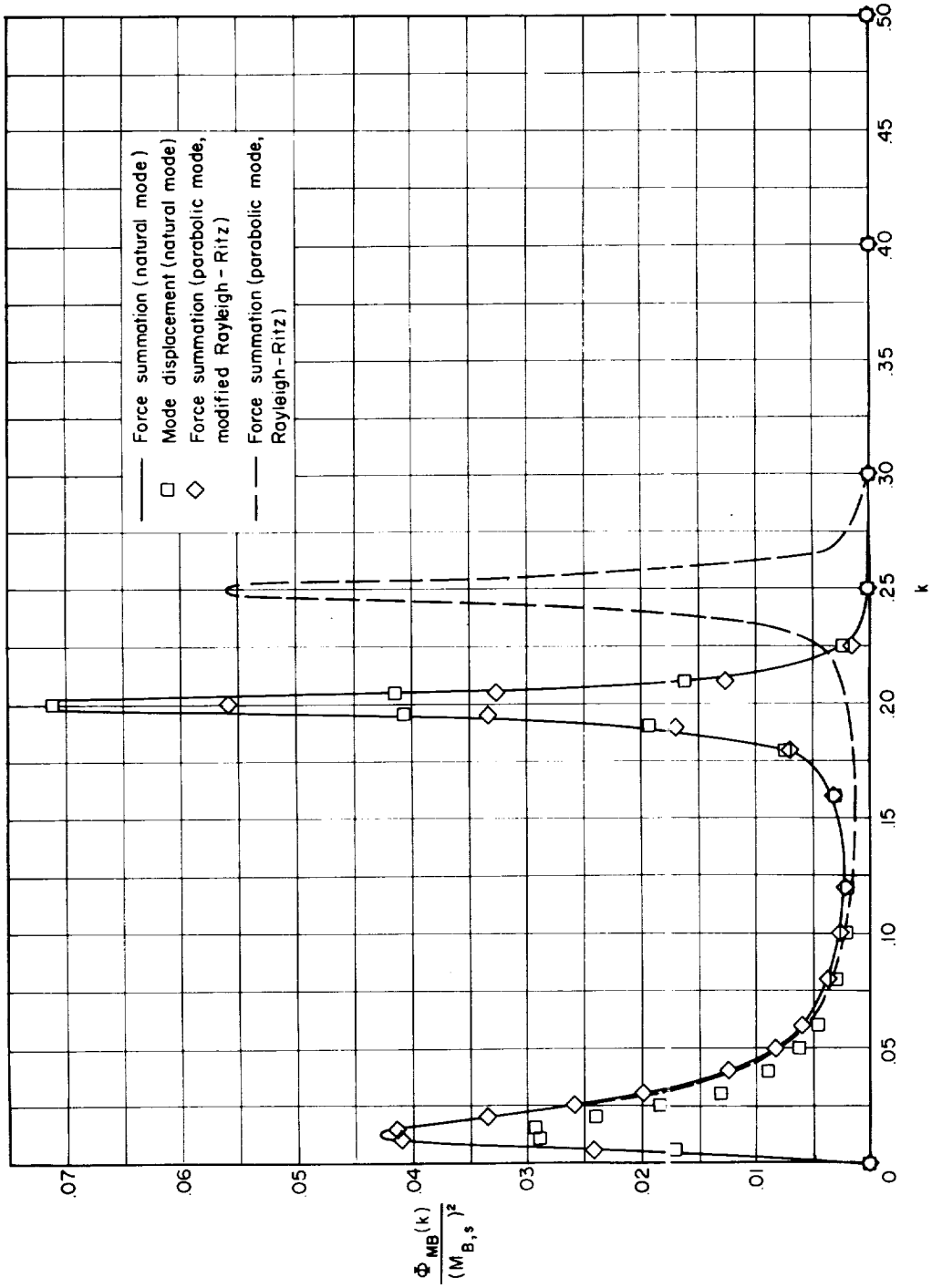

(a) Output bending-moment spectra for one-dimensional turbulence. $\mu = 0.5$; $\bar{y}_1 = 0$.

Figure 5.- Evaluation of several simplified modal methods by spectra comparison.

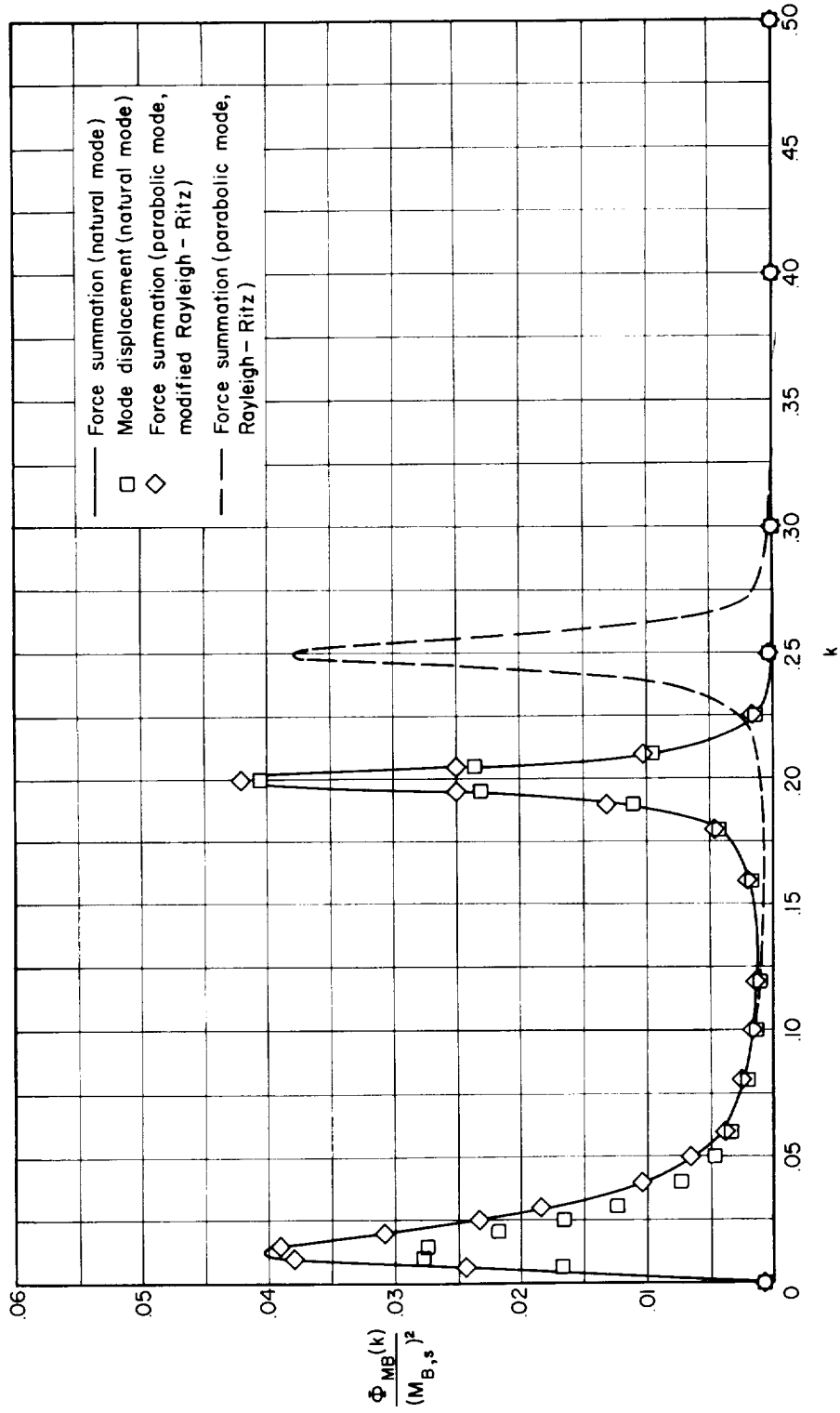

(b) Output bending-moment spectra for two-dimensional turbulence. $\mu = 0.5$; $\bar{y}_1 = 0$.

Figure 5.- Continued.

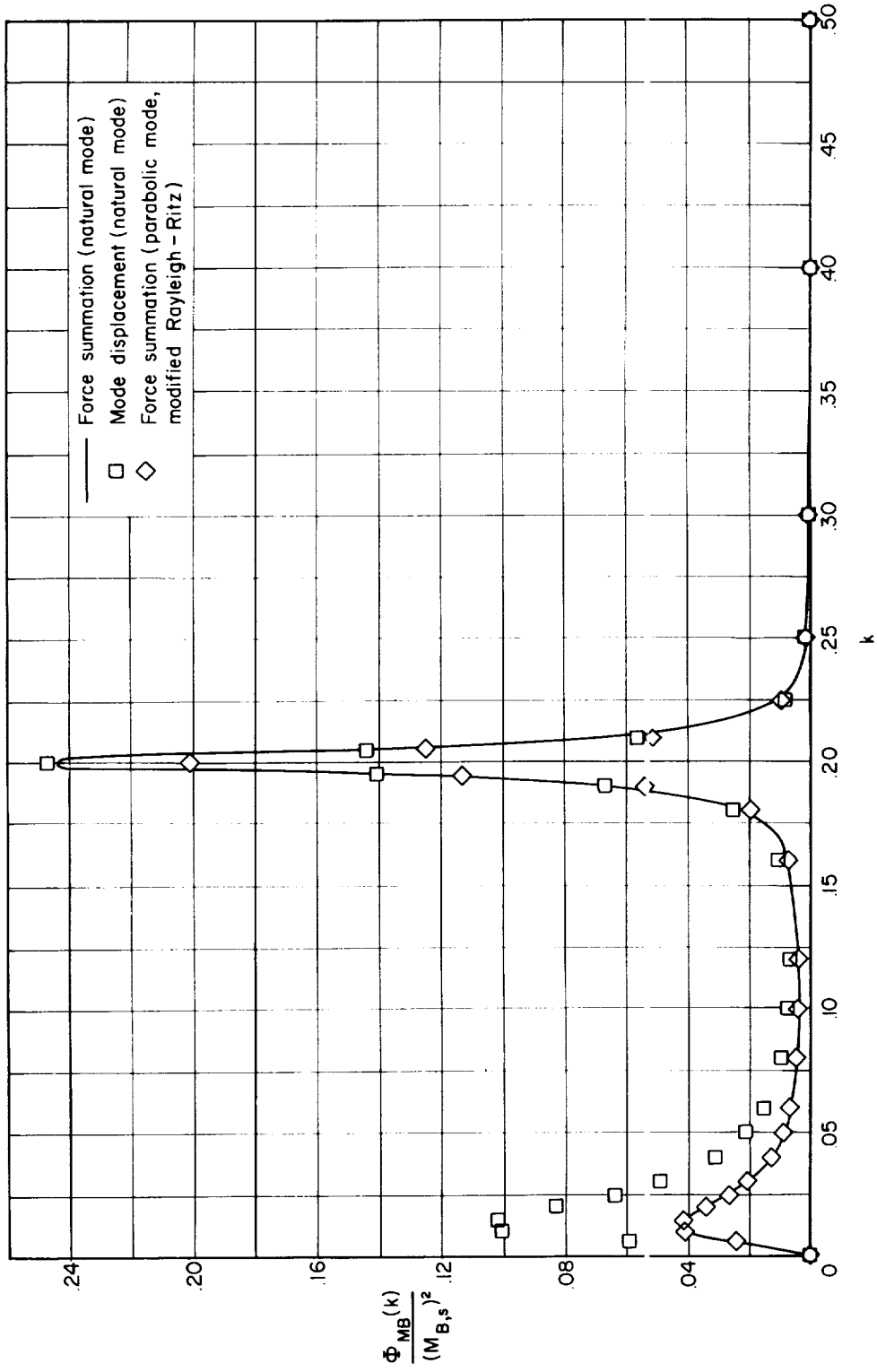

(c) Output bending-moment spectra for one-dimensional turbulence. $\mu = 0.5$; $\bar{y}_1 = 0.75$.

Figure 5.- Continued.

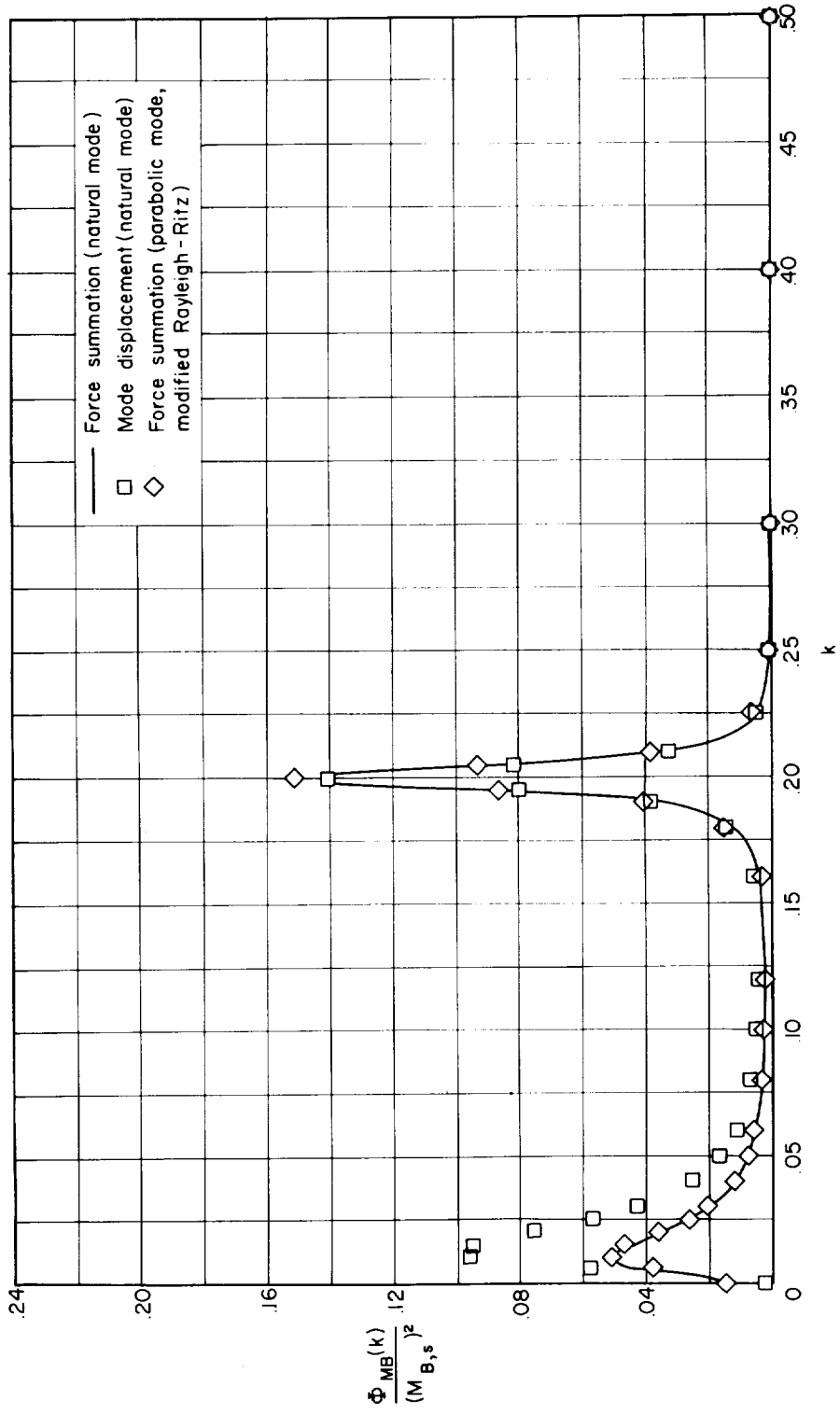

(d) Output bending-moment spectra for two-dimensional turbulence. $\mu = 0.5$; $\bar{y}_1 = 0.75$.

Figure 5.- Concluded.

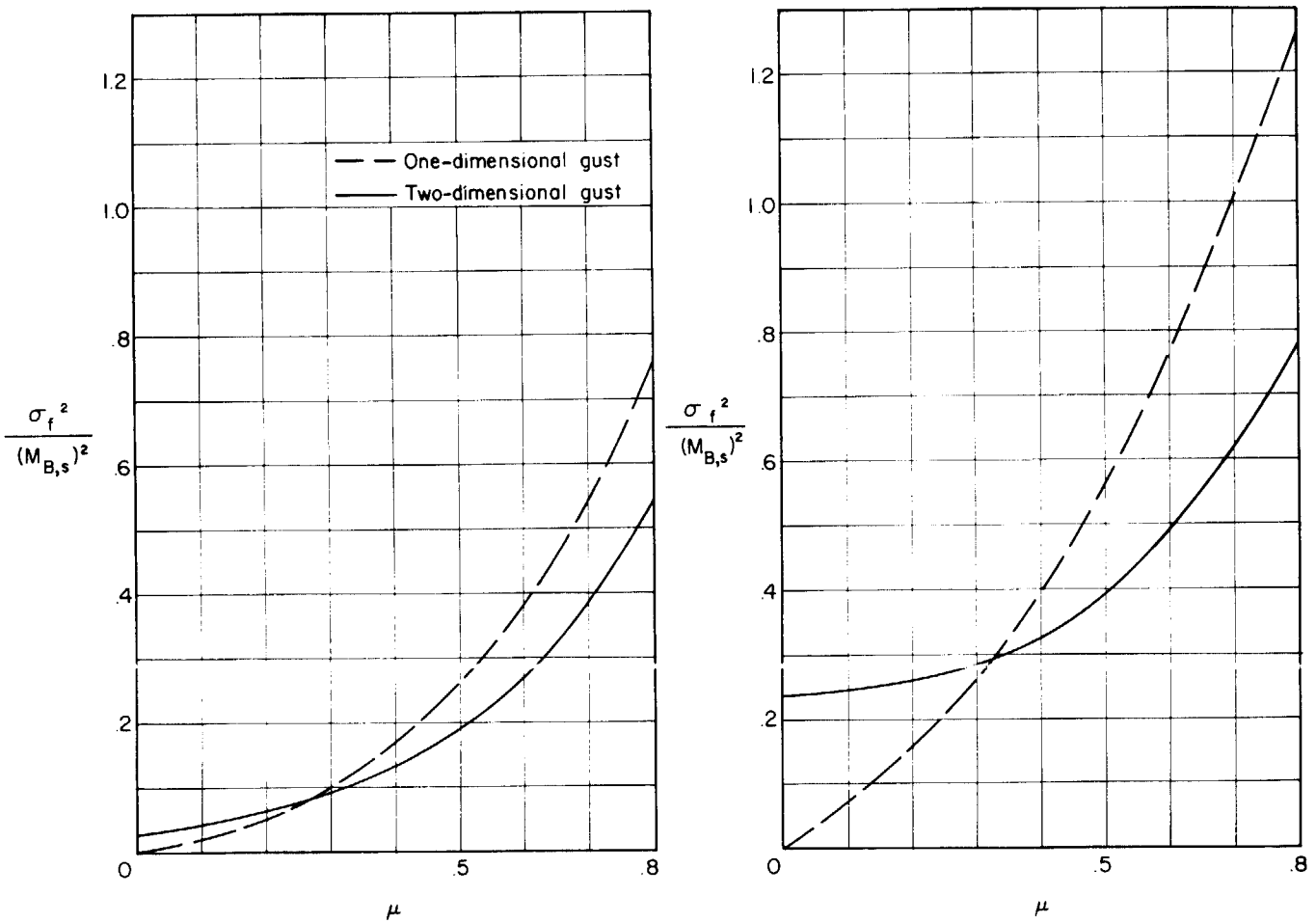

(a) $\bar{y}_1 = 0$; exact method.

(b) $\bar{y}_1 = 0.75$; force-summation method.

Figure 7.- Comparison of mean-square bending-moment response for one- and two-dimensional turbulence.

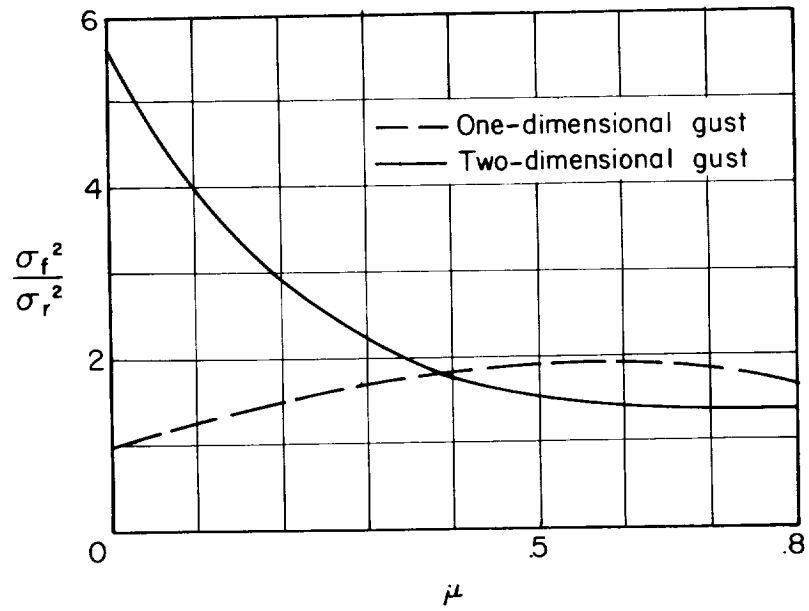

(a) $\bar{y}_1 = 0$; exact method.

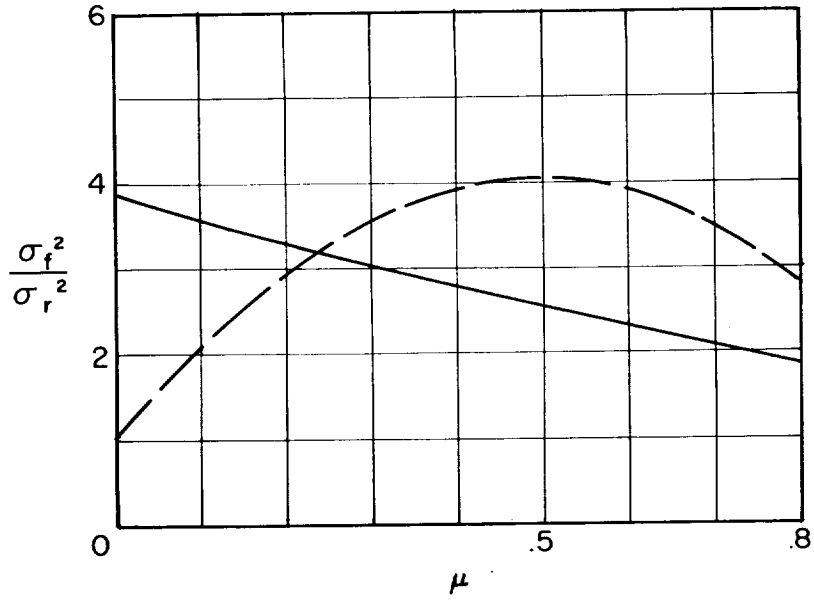

(b) $\bar{y}_1 = 0.75$; force-summation method.

Figure 8.- Comparison of mean-square bending-moment ratio for one- and two-dimensional turbulence.

NASA - Langley Field, Va. L-143